A Simple Model of Crowdfunding Dynamics*

Matthew Ellman† and Michele Fabi‡

Incomplete draft

September 2019

Abstract

This paper develops a dynamic game with endogenous inspection costs to explain empirically salient bidding profiles in crowdfunding and to characterize how success rates vary with design parameters. In the baseline, bidders arrive at a constant rate and face an inspection cost to learn if they like the crowdfunder's product. The average funding profile is weakly decreasing over time for any fixed inspection cost. Heterogeneity and a relatively high threshold can generate an increasing bid profile: only low inspection cost types inspect at first but their bids tend to convince higher types to start inspecting over time. The addition of a group of contacts who can bid on the project at the start of the campaign can give rise to a bimodal or U-shaped profile. We also derive a U-shape without this but the conditions are more restrictive. Moreover, to explain a more pronounced final peak or upturn in the U-shape, we extend to allow for endogenous timing by letting some bidders choose to wait before inspecting. We also study how conditioning on project success or failure affects funding profiles and solve a continuous-time version of the model. We conclude with implications for success rates and lessons for optimal design.

JEL Classifications: D26, C73, L12.

*We thank Sjaak Hurkens, Carolina Manzano Tovar, Antonio Miralles for valuable discussions, together with participants at WIPE (Reus, 2019), EARIE (Barcelona, 2019) and JEI (Madrid, 2019). We also gratefully acknowledge financial support from the 2016 FBVVA grant "Innovación e Información en la Economía Digital," the Severo Ochoa Programme for Centres of Excellence in R&D (SEV-2015-0563), the Spanish Ministry ECO2017-88129-P (AEI/FEDER, UE), Ellman; FPI fellowship 914886-79792965, Fabi) and the Generalitat of Catalunya (2017 SGR 1136).

†Institute of Economic Analysis, IAE-CSIC, and Barcelona GSE (matthew.ellman@iae.csic.es)

‡Universitat Autónoma de Barcelona, IDEA-UAB, and Barcelona GSE (michele.fabi@e-campus.uab.cat)

1 Introduction

A growing wealth of crowdfunding data has led empiricists to highlight a salient U-shaped time profile of pledges from funders, but we lack a solid dynamic theory capable of explaining the stylized facts. Early models of crowdfunding simply neglect dynamic issues by assuming simultaneous bidding. Understanding the dynamics is vital for entrepreneurs who want to limit the risk of funding failure and for platforms that want to attract both entrepreneurs and funders. We construct a parsimonious model that can generate a U-shaped profile, while also characterizing bidding patterns and project success rates for a range of simple environments.

The model is based on two central features of reward-based crowdfunding: inspection costs and thresholds. In reward-based crowdfunding, the funders who bid on a project are rewarded with the entrepreneur's product(s) if the campaign succeeds. We study the dominant all-or-nothing format where rewards are only produced if aggregate funds pledged during the campaign reach the entrepreneur's goal or *threshold*; if the project fails, nothing is produced and all bids are returned. Crowdfunding obliges entrepreneurs to solicit bids *before* production so consumers face higher *inspection costs* than for a pre-existing product. Moreover, these costs interact with the threshold because bidders gain nothing from inspecting projects that fail to reach their funding thresholds. We endogenize inspection and bidding and we show how inspection costs interact with the threshold to determine a project's evolving success rate.

We begin the paper with a novel characterization of bidding profiles on a single project in a setting where each bidder decides whether to inspect and bid in the same period in which he "arrives," that is, comes across the project. In this setting with a fully "exogenous" move order (called the "exo" model), there is some tendency towards a decreasing bid profile, but certain parameter specifications generate increasing profiles and U-shaped profiles. After explaining the origin of those results, we introduce endogeneity in move order by allowing bidders to set an alert or alarm to revisit the project at a later moment to see how bidding evolved. That "endo" model is capable of explaining sharper increases in bidding near to the project deadline and near to the date at which the project reaches its threshold. Finally, we depart slightly from our assumption of a constant bidder arrival rate to allow for a bunch of arrivals at the beginning, based on the logic that some consumers, such as the entrepreneur's contacts, fans and friends, become aware of the project before its formal launch as an active crowdfunding campaign. We then discuss implications of various extensions of the model and alternative approaches. We (will) close with an analysis of implications for optimal design.

In our simplest setting, bidders have homogenous inspection costs and the bid profile, measured as the average rate of bidding, is decreasing over time, given the assumed constant bidder arrival rate. Consider a bidder who arrives and observes that there are r periods remaining and a gap g between the threshold and funding so far. The success rate S at this node is decreasing in the gap g and the remaining time r in which other bidders can arrive and help to bridge the gap. If the success rate is high enough relative to the bidder's inspection cost c, the project is "hot" in that all bidders will inspect and bid if they like the product. Otherwise, the project is "frozen" in that no bidders will inspect and the project is bound to fail. In this simple case, there are just two heat states and the frozen state is an absorbing state, whereas the hot state only becomes an absorbing state ("boiling") if the gap falls to 1. As a result, for thresholds

strictly above one, the probability that the project is frozen increases over time. This generates a decreasing average bid rate. Moreover, conditioning on success, the average bid rate is still decreasing even though the averaging now places weight only on (r, g) paths that avoid freezing. This is because enough bids must occur early enough during the campaign to avoid freezing. We explain this more clearly in terms of heat contours, but first describe the simplest two period case.

The intuition can be seen in a two-period crowdfunding campaign, with one funder arriving in each period. With a zero inspection cost, the (average) bid profile is flat: both funders inspect and pledge if they like the good. A flat profile is equally immediate in the opposite case where the inspection cost is so high that even funder 1, the early funder, does not inspect. Funder 2 then never inspects either and the campaign is doomed to fail. The intermediate case with a moderate, positive inspection cost and a threshold of two provides the only non-trivial slope.[1] A success then requires both funders to bid, funder 1 always inspecting while funder 2 doing so only if funder 1 contributes. In expectation, bids in period 2 are lower. Allowing bidders to wait, the model predicts a null or increasing bid profile for two-period or three-period campaigns. Indeed, if only two bidders become sequentially aware and two bids have to be collected for success, the last to become aware never waits. The first instead chooses to arrive in the last instant as long as the chances of success are positive. Keeping a goal of two and adding another period, we can have either a dead profile or an increasing profile, with only the first bidder waiting for a low and positive inspection cost, the first two for a moderately high cost, and all abstaining for a higher cost that makes success impossible. In general, homogeneous inspection cost and endogenous timing give rise to an increasing profile for a moderately high inspection cost, characterised by a period of initial delay, a gradual rise in the bid rate and a final peak.

A central distinguishing feature of our approach is the analysis of heterogeneous inspection costs.[2] Heterogeneity permits us to generate interesting dynamics even with exogenous arrivals and fixed pre-purchase price. Assuming heterogeneity, a variey of profiles can be obtained. A simple form of binary heterogeneity allows the model to predict an increasing profile. To fix ideas, consider again the two-period example examined before with a threshold of 2 in the case where bidders have either $c_L = 0$ with probability z and otherwise $c_H > 0$. Suppose initially that any L-type inspects on arrival and bids if he likes the good, even on arriving in period 2 and observing no prior bid. If c_H is so high that H-types never inspect, we are back to the case of a flat profile, but the profile is non-trivial if c_H is moderately high. Then an H-type bidder 1 does not inspect while an H-type bidder 2 inspects *conditional* on observing a bid by bidder 1. Thus, bidder 1 inspects (and potentially bids) only if he is an L-type, while bidder 2 inspects both if L-type *and* also in the case of an H-type if bidder 1 bids. So bids in period 2 are higher in expectation. We refer to this case as a "cold start" because the project's chances of success are too low to induce inspection by the H-types at the beginning.

The profile's slope is inverted in the case of a "hot start", i.e. where both types of bidder

[1] If the threshold is one or zero, either all funders inspect and the bid profile is flat (with a positive average), or none of them do so and the bid profile is flat (at zero). A threshold strictly exceeding two or a high cost leads to the latter case (flat at zero). A zero cost leads to the former case (all funders inspect).

[2] They appear different because the assumed bidding costs are from "tying up funds" but the critical difference is that all those papers, discussed below, assume homogeneous bidding costs.

always inspect at the beginning. This arises when c_H is low enough for bidder 1 to inspect regardless of his type, while a H-type bidder 2 only inspects conditional on observing that bidder 1 contributes. As a result, bids decrease in expectation, as with homogeneous inspection costs. When the frequency of bidder arrivals increases, we find that the heating effect is robust if the campaign is sufficiently cold and the arrival rate low. Conversely the cooling effect produced by after a hot start is not robust and arises only for a narrow and vanishing region of positive inspection costs. When timing is endogenous, we obtain a U-shape combining initial bunching of contacts and friends with gradual heating effect. In the case of a cold start, a time-decreasing bid rate accompanied by the heating effect produce a smooth increase in bid rates that culminate in a final contribution peak.

When each bidder's inspection cost is uniformly distributed, the bid profile is decreasing over time. This occurs because current bidders see the next period from the optimistic view of good news that they pledge. The next arriving bidder however can find himself in a scenario where his predecessor did not pledge which would reduce the bid rate. This strength of this effect increases in a bidder's pivotality. Adding an atom at zero only attenuates this effect but does not shift the profile's monotonicity. On the other hand, using a quadratic (and hence convex) c.d.f., we find configurations of parameters that produce an increasing profile adding a large enough atom at zero, which causes the same gradual heating effect already presented for the case of binary inspection cost.

The overall picture we get is that it is difficult to predict U-shape with exogenous arrivals because, in general, it is hard to have an increasing bid rate with that increase sharply towards the end. On the other hand, when awareness is exogenous and arrival endogenous, the story is the opposite.

Other alternative and complementary theories can provide a plausible explanation for the emergence of the U-shape. The first relies on a common value, endogenous timing model: bidders receive signals of different value and precision and decide whether and when to bid. Early bidding is generated by those who receive positive and precise signals; late bidding is driven by those who receive imprecise signals and wait for the campaign to progress and infer the quality of the product looking at past bidding. If the campaign is likely to be successful, many bids are collected, and the posterior on the project's quality increases up to the point that can lead to the formation of cascades. On the other hand, bidders who receive negative and precise signals never bid. An alternative approach is based on a private values, endogenous timing and endogenous inspection model. Allowing bidders to choose in which period they inspect (and consequently bid), the least-cost bidders bunch at the beginning self-selecting themselves as promoters of the campaign while higher-cost bidders delay their inspection until it becomes clearer whether the project will succeed becoming followers. Another compelling alternative relies on a model of advertising and strategic prominence determined by the entrepreneur and the platform. High and low momentum phases may reflect different intensities of attention that the project receives. The initial peak of the U-shape occurs because of a higher intensity of promotion by the entrepreneur; with a strong enough kick-start, the size of the supporting community may grow over time leading pledges to gradually increases.

We will show how the threshold alone can generate a range of dynamic effects that will

continue to be relevant in richer models. Advertising and platform promotion strategies represent an unquestionably important part of the puzzle, but to derive the optimal promotion strategies, we first want to know how the dynamics of campaigns respond to an exogenous bidder arrival rate. Other forces, such as word-of-mouth learning and common value effects, can have a strong influence on the observed funding patterns, but we have shown that the current model is simple enough to account for the most salient facts, generating a U-shaped profile, as well as increasing and decreasing patterns, depending on the project's starting condition and the distribution of inspection costs. Since the threshold matters even without any of these additional effects, we start from there, providing a parsimonious model that can fill a basic gap of this literature.

The rest of the paper is organized as follows: The literature review is discussed in Section 1.1. In Section 2, we present the baseline model with exogenous timing of arrival. In Section 3.1 we prove existence and uniqueness of the equilibrium and other basic monotonicity properties. In Section 3.2 we provide conditions for determining the sign of the slope of the bid rate profile, and we study how its monotonicity is affected by making different assumptions on the distribution of inspection costs in Section 3.3, 3.4 and 3.5. In Section 4 we extend the model introducing endogenous timing. We conclude in section Section 5. Appendix A presents the methodology employed to derive the model in continuous time.

1.1 Related literature

The literature on crowdfunding models began with Belleflamme et al. (2014), followed by (Ellman and Hurkens, 2019b,a; Hu et al., 2015; Strausz, 2017; Chang, 2016; Chemla and Tinn, 2018), most of which are static and sometimes extended to a two or three-period setting. They cover topics such as campaign design (Ellman and Hurkens, 2019b; Chang, 2016; Belleflamme et al., 2014; Hu et al., 2015), moral hazard (Ellman and Hurkens, 2019a; Strausz, 2017; Chang, 2016; Chemla and Tinn, 2018), demand learning (Ellman and Hurkens, 2019b; Chang, 2016). An early discussion on the economics of crowdfunding that anticipated this stream of literature is provided by Agrawal et al. (2014).

Empirical and studies proliferated along with theoretical analyses. (Agrawal et al., 2011) is an early study of the geographical distribution of backers' and the timing of their pledges. They find that pledging propensity increases as the campaign accumulates capital, and finds an inverse relation between proximity to the entrepreneur and time of bidding.

Other authors, (Kuppuswamy and Bayus, 2017; Crosetto and Regner, 2018; Rao et al., 2014) use daily data to study the determinants of pledge dynamics. (Kuppuswamy and Bayus, 2017; Crosetto and Regner, 2018) find evidence of the U-Shape (or bathtub) pattern of pledges in the platforms Kickstarter and Startnext. This pattern is characterised by funding peaking initially and towards the end of the campaign, following a lull in pledges during the middle phase. Regarding the composition of the U-shape, these authors find that self-bidding and bids from the entrepreneur's personal connections mostly occur within peaks. On aggregate, the U-shape is pervasive across project types and categories, regardless of the campaign's outcome, but at the campaign level, Crosetto and Regner (2018) find that the U-shape hides large heterogeneity. Also working at the campaign level, Kuppuswamy and Bayus (2017) find that pledging drops after the goal is reached. Rao et al. (2014) build a predictor of success based on pledge inflow

and its first derivative. They find that pledging occurring within the initial 10% and between 40% and 60% of the funding period and the first derivative during the concluding 5% of the funding period have the strongest impact in predicting success. Also, they find that a predictor based on the inflows during the initial 15% of the campaign predicts success with 84% accuracy. This finding is in line with Crosetto and Regner (2018), who also find that abundant early seeding is a good predictor of success, but find that its lack does not imply failure. Under track campaigns are often saved by a large pledge resulting from intensified communication effort or support from the entrepreneur's extended personal network. (Colombo et al., 2015) find that substantial pledging in the starting days of a campaign is positively related to the presence of internal social capital developed within the crowdfunding community.

(Mollick, 2014; Cordova et al., 2015) use project-level datasets to study static characteristics of successful crowdfunding practices. Mollick (2014) use a sample of Kickstarter, while Cordova et al. (2015) restricts the sample to technology projects active in 2012 combining the two leading U.S. based platfom, Kickstarter and Indiegogo, the Italian Eppela, and the European oriented platform Ulule. Both authors find bimodality in revenues and completion times. They also agree that higher goals are associated with lower success rates, but disagree on whether larger durations are associated with higher Cordova et al. (2015) or lower Mollick (2014) success rates. (Moritz and Block, 2016; Short et al., 2017; Kuppuswamy and Bayus, 2018) present a literature review of the empirical and management literature on crowdfunding. Overall, none of the aforementioned studies provides a detailed analysis of how the bid profile varies based on project's characteristics.

A more recent literature explicitly models pledging resulting from a dynamic contribution game. Alaei et al. (2016) is a solid operations research paper that studies optimal crowdfunding design and explain bimodality in revenues as a result of cascading behavior. It assumes bidders arrive exogenously and face an opportunity cost of pledging when the project fails. Each bidder valuation is ex-ante stochastic and drawn a binary distribution. Bidder's estimates of success are determined using the anticipating random walk process. Alaei et al. (2016) does not focus on studying the bid profile, which is necessarily decreasing in their setting.

Deb et al. (2018) model the U-shape as a result of purchases and donations from exogenously arriving buyers and just one donor endogenously choosing when and how much to contribute. There is a multiplicity of equilibria but they make predictions by restricting attention to the unique one that is platform (and donor) optimal. Buyers are homogeneous and face an opportunity cost when the campaign fails, as in (Alaei et al., 2016). Stochastic bid dynamics are the result of assuming a stochastic arrival rate and buyers' uncertainty about the donor's valuation of success. The donor is a necessary element for this model to generate U-shape dynamics. The profile would always be decreasing without her. Our model based on inspection costs avoids the need to assume the presence of a donor. That is, we predict a U-shape when all bidders are ex-ante alike. Donor motives are certainly relevant in a number of crowdfunding settings, but it introduces technical complexities that oblige Deb et al. (2018) to assume just one donor. Moreover, to understand what is caused by donor motivations, we need to know what bidding profiles can be explained in a model with ex-ante symmetry among the funders. In terms of parsimony, it is also notable that we can generate a range of profiles via cost uncertainty alone and we achieve stochastic dynamics from the taste shock alone, without need for stochastic

arrivals. Deb et al. (2018) is a valuable complement to our simpler and symmetric setting.

Other related works (Zhang et al., 2017; Chakraborty and Swinney, 2018; Du et al., 2017) offer a mix of interesting insights but do not provide a complete model of bid dynamics to explain bid profile data. Zhang et al. (2017) assume bidders are divided into ordinary (early) bidders and herding bidders, who pledge at the campaign's deadline only if the project is successful. They do not model bidders' choice between being early bidders or herders. In Chakraborty and Swinney (2018), bidders arrive sequentially and do not take time into account when making their decision to pledge. Their model can only predict flat or increasing profiles (flat with possibly a spike at the end). Du et al. (2017) study three form of contingent stimulus policies; that is, seeding via free samples, product upgrades and other time limited offers. They do not provide a clear profile prediction, only explicitly treating the case of bidders unaffected by funding dynamics or behaving as if they had homogeneous inspection costs. Again that forces a decreasing profile in the absence of stimulus policies.

Common values offer another promising avenue for understanding dynamics. Given the prominent role of thresholds and limited campaign duration in actual crowdfunding, it will be important to combine common values with the model that we develop below. Nonetheless, there are already some suggestive early contributions. Liu (2018) studies endogenous formation of leaders and followers in models of learning and collective investment. She studies a two-period game assuming common value and endogenous move order. Of course, that precludes explaining a U-shape and other possibilities. Her game always has an equilibrium such that the profile of successful campaigns is increasing while that of failed campaigns is decreasing, but it can have multiple equilibria, so it needs to be refined to provide a clear characterization of the bidding profile. Babich et al. (2017); Vismara (2016); Zhang and Liu (2012) provide valuable related contributions in the context of equity-based crowdfunding.

Finally, there are several papers on donation-based crowdfunding. Solomon et al. (2015) study the timing of pledges experimentally. Donors tend to bunch their pledges at the beginning and at the end of a campaign. In line with our findings on endogenous timing, early pledging is a better strategy for donors who value success. Cason and Zubrickas (2018) study both theoretically and experimentally the impact of refund bonuses on the provision of public goods. In their dynamic contribution game, bidders can pledge more than once to a public good in continuous time. They find that refund bonuses help coordinate bidders and reduce contribution momentum but they make no clear predictions on bidding dynamics.

Our study is more distantly related to models of bargaining or irreversible investment in continuous time with endogenous move order. Zhang (1997) studies investment cascades over a finite horizon in continuous time. In his set-up, the first contributors with high precision signals revel all information; all other bidders pledge right afterwards because there is no value in waiting. On the other hand, Ma and Manove (1993) claim the opposite result in a model of bargaining with deadline and strategic delay, assuming bidders have imperfect control over the time they pledge because of a buffering period. In their model, successful offers are accepted in proximity of the deadline. Finally, a promising next step would be to bring mechanism design to bear on our question. Shen et al. (2018) study information design in crowdfunding. Their focus is on the value of strategic delay in disclosing information about bidding.

2 Model with exogenous timing

We study the simplest reward-based crowdfunding project. An entrepreneur creates a project to make a single product. A consumer is a bidder if he "arrives" or hears about the project before its deadline. He can then bid to pay the crowdfunding price p. If the project succeeds, denoted $\mathcal{S}$, in accruing at least K bids by the deadline T, bids are paid, production occurs and rewards are delivered. If the threshold K is not reached by T, the project fails, denoted $\mathcal{F}$, bids are reimbursed, there is no production and no rewards (the crowdfunding paradigm is "All-or-Nothing").[3]

A bidder arrives in each period $t \in \{1, \ldots, T\}$ of the crowdfunding campaign with probability $\lambda \in (0, 1]$.[4] We focus on $r \triangleq T - t + 1$, the "*rem*" or number of periods remaining before the campaign deadline and use r to label a bidder arriving with rem r. Any such bidder must pay an inspection cost if he wants to learn his value for the product (the "reward"). Otherwise he only knows the prior distribution: his value is $v > 1$ with probability $q \in (0, 1)$ and 0 with probability $1 - q$, resale being impossible. For concreteness, we suppose that *after* production occurs in successful crowdfunding, consumers observe their value at no cost but the entrepreneur then sells her product at price v, yielding no consumer rent from ex post purchases. In crowdfunding, the entrepreneur must offer a discounted price $0 < p = v - d < v$ to induce the sunk cost of inspection since $q < 1$. So the discount is $d \in (0, v)$. Inspection costs and bidders' values are mutually independent and independent across bidders. As just noted, bidder values v_r are drawn from the Bernoulli distribution $(v, q; 0, 1 - q)$. Inspection costs c_r are drawn from the cumulative distribution function $F(.)$ with support $[0, q]$.[5]

In the baseline, each bidder either ignores the project or decides on inspecting and bidding, without considering the option of delaying to see how the campaign progresses and acting at that later date prior to the deadline. That is, he chooses inspect or not and bid or not in the exogenous period of arrival; we call this the "exo" model. It does allow a bidder who chooses A at r to buy ex post if production occurs but then the rent is zero. On top of the common prior on project characteristics (T, λ, q, v), when bidder r arrives, he observes: (i) the rem r of periods left (equivalent to observing t), (ii) the gap g between the bids collected so far and the threshold K (equivalent to observing the interim bids collected) and (iii) his inspection cost c_r.[6] His full type is (v_r, c_r) but he only observes v_r if he inspects.

Every period consists of two sub-stages: if a bidder arrives at r, he chooses, (i) whether to inspect, paying c_r and acquiring a perfect signal of his taste v_r, (ii) whether to bid, based on his

[3] Bidder threshold K can also be expressed as aggregate fund threshold Kp

[4] λ is initially constant but later we allow multiple arrivals in the initial period; that initial bunch reflects how a stock of bidders ("contacts") may learn about the project before the campaign is formally initiated. When studying the continuous time limit, we denote the project duration by τ and divide each time unit into $n \in \mathbb{N}$ periods, so that there are $T = n\tau$ periods and the per-period arrival probability is $\lambda = \frac{\tau\mu}{n}$.

[5] This is without loss of generality: first, bidders with negative inspection costs, perhaps reflecting curiosity in the project, would behave exactly as do 0-cost types; second, a positive mass on $c > q$ is equivalent to lowering the rate of bidder arrival (that is, in the notation just below, lowering λ to $\lambda(1 - F(q))$ while replacing $F(c)$ by $F'(c) \triangleq F(c)/(1 - F(q))$ on the restricted support $c \leq q$).

[6] In the baseline, we will show that it does not matter whether bidder r observes the breakdown of prior bids or gap path $(g_s)_{s \geq r}$, nor the inspection costs of prior bidders $(c_s)_{s \geq r}$, but those distinctions do prove important in the endogenous timing model. For example, if later bidders knew that earlier bidders who did not bid had zero inspection costs, they would infer that those bidders do not value the good and will never bid.

realised signal if he inspected. It is clearly dominated for a bidder at r to inspect after bidding or to inspect if he will then disregard or bid against his signal, so we need only consider three (compound) choices: **A**bstain from bidding, **B**lind bid (bid without inspecting), **C**heck (inspect and bid if $v_i = v$ is learnt), denoted A, B and C. A generic bidder strategy is then a mapping from each possible rem, gap, cost, (r, g, c_r) to this trinary set of choices. The nodes of the game are $(r, g) \in \{0, \ldots, T\} \times \{K - T, \ldots, K\}$. A bidder arrives with probability λ in any $r > 0$. Rem $r = 0$ represents the end of the campaign so it is just too late to bid at $r = 0$, but the gap g_0 determines whether the project succeeds: $\mathcal{S} \equiv g_0 \leq 0$. This represents the fact that the funding gap falls from K to 0 or below before time T runs out. A failure $\mathcal{F}$ arises in the complementary event that the gap ends at some $g_0 > 0$. Since c_r has no impact on r's payoff from A and B but strictly reduces the payoff from C, we can define the "heat" $h_{(r,g)}$, of the campaign at a given node, by the highest type willing to choose C there. For a continuum of types, $h \in [0, q]$. For a J-type discrete distribution, $c_1 < c_2 <, \ldots, < c_J$, we define the state j such that all types $i : c_i \leq c_j$ choose C while higher types choose A. There are then $J + 1$ heat states: $\varnothing, 1, \ldots, J$ where state $\varnothing$ is the frozen state in which no type wants to inspect. The frozen state never occurs if $c_1 = 0$.

Bidder r's ex-post payoff from choice A is simply $u^A = 0$. In choice B, bidder r purchases the good blindly in that he risks buying a product that he does not value.

$$u^B = \mathbb{1}_{g_0 \geq 0} (v_r - (v - d)) \tag{1}$$

If r opts for choice C, he pays c_r and buys the good only if he values it ($v_r = v$).

$$u^C = \mathbb{1}_{g_0 \geq 0} (v_r - (v - d))^+ - c_r \tag{2}$$

When bidder r observes (r, g), his expected utilities from B and C are therefore

$$U^B_{(r,g)} = \mathbb{E}_{(r,g;b_r=1)}[\mathbb{1}_{g_0 \leq 0}] (d - v(1 - q)) \tag{3}$$

$$U^C_{(r,g)} = q\mathbb{E}_{(r,g;b_r=1)}[\mathbb{1}_{g_0 \leq 0}] d - c_r \tag{4}$$

To restrict the analysis to cases where bidders never play B, keeping d constant and normalized at 1, we assume that the prior on liking the good is sufficiently low so to discourage them to take the chance and buying without inspecting:[7]

Assumption 1 (No blind bidding). $q < 1 - 1/v$

Finally, we resolve indifference between C and A in favour of inspection and production by assuming that bidders then choose C.

The gap shrinks over time, and it drops from round r to $r - 1$ by the amount of bids collected at r,

$$g_{(r-1)} = g_{(r)} - b_{(r)} \tag{5}$$

[7] An alternative normalization is to set $v = 1$. In this case assumption: 1 becomes $q < 1 - d$.

Given at most one arrival in round r, the gap either falls by one or remains unchanged,

$$g_{(r-1)} = \begin{cases} g_{(r)} & \text{if } b_r = 1 \\ g_{(r)} - 1 & \text{if } b_r = 0 \end{cases} \tag{6}$$

Thus, when the campaign reaches node $(r, g_{(r)})$, the expected change in gap is

$$\mathbb{E}_{(r,g_{(r)})}\left[g_{(r)} - g_{(r-1)}\right] = p_{(r,g_{(r)})} \tag{7}$$

where $p_{(r,g)}$ is the probability of a bid at node (r, g). .

To study the time profile of bids, we will be looking at how the bid rate varies across periods, taking expectation over possible realizations of the gap. We obtain the (unconditional) bid rate in period r by averaging-out $g_{(r)}$, taking expectation over the (conditional) bid rates at nodes $(r, g_{(r)})$ for all $g_{(r)}$. Also, to study how the profile varies depending on the campaign's outcome, we restrict the sample space to gaps that are on successful or failed paths. A key object is the probability of success for a campaign at node (r, g). We denote this interim success rate by $S_{(r,g)} \triangleq \mathbb{E}_{(r,g)} \mathbb{1}_{g_0 \leq 0}$ and similarly the success rate from the point of view of a funder bidding at (r, g) by $S'_{(r,g)} \triangleq \mathbb{E}_{(r-1,g-1)} \mathbb{1}_{g_0 \leq 0}$. With a slight abuse of notation, we denote the ex-ante success rate as $S_{(T,K)} \equiv S$.

Letting $P_{(r,g)} \triangleq \mathbb{P}(g_{(r)} = g) \equiv Q_{(r,g_{(r)};T,K)}$ denote the probability of reaching node (r, g) from the initial node (T, K), we pin-down the aggregate and conditional bid rates as follows:

$$A_r = \sum_{g=K-(T-r)}^{K} P_{(r,g)} p_{(r,g)} \tag{8}$$

$$A_r^{\mathcal{S}} = \frac{1}{S} \sum_{g=K-(T-r)}^{K} P_{(r,g)} \left[p_{(r,g)} S_{(r-1,g-1)}\right] \tag{9}$$

$$A_r^{\mathcal{F}} = \frac{1}{1-S} \sum_{g=K-(T-r)}^{K} P_{(r,g)} \left[p_{(r,g)} (1 - S_{(r-1,g-1)})\right] \tag{10}$$

The formulas in Eqs. (58) to (60) can be computed exploiting the recursive definition of $S_{(r,g)}$ and $P_{(r,g)}$:

$$\begin{cases} S_{(r,g)} = p_{(r,g)} S_{(r-1,g-1)} + (1 - p_{(r,g)}) S_{(r-1,g)} \\ S_{(0,g)} = 1 \text{ if } g \leq 0 \\ S_{(0,g)} = 0 \text{ if } g > 0 \end{cases} \tag{11}$$

and

$$\begin{cases} P_{(r,g)} = P_{(r+1,g+1)} p_{(r+1,g+1)} + P_{(r+1,g)} (1 - p_{(r+1,g)}) \\ P_{(T,K)} = 1 \end{cases} \tag{12}$$

Note that the end-point conditions for $S_{(r,g)}$ are specified at the end of the campaign while those of $P_{(r,g)}$ at the beginning. This implies that the two objects are determined through a backward and forward iteration. For a graphic depiction of the paths over which this averaging

takes place, see Fig. 12.

In the next section we derive the basic equilibrium properties for the model with exogenous arrivals, assuming at most one potential bidder in all periods except the start.

3 Analysis

3.1 Basic equilibrium properties

Using the model defined in section 2, we analyse the bidding profile that emerges from the equilibrium bidding strategies.

When at most one bidder at most arrives each period, the game has a unique PBE in threshold strategies: bidders play C if their inspection cost is below a given threshold $\hat{c}_{(r,g)}$.[8]

Proposition 1 (Existence and uniqueness of the equilibrium). *The game defined in section 2 has a unique PBE such that bidders play C if and only if $c_r \leq \hat{c}_{(r,g)}$, defined as*

$$\hat{c}_{(r,g)} \triangleq qS_{(r-1,g-1)} \tag{13}$$

where $S_{(r-1,g-1)}$ are given by the Eq. (11)

Proof of Proposition 1. In Appendix C ■

As a consequence of Proposition 1, $p_{(r,g)}$ is given by

$$p_{(r,g)} = \lambda F(\hat{c}_{(r,g)})q = \lambda F(qS_{(r-1,g-1)})q \tag{14}$$

and we can define heat as

$$h(r,g) \triangleq arg\max_j : c_j \leq \hat{c}_{(r,g)} \tag{15}$$

Before examining the dynamic bidding profile, we provide an auxiliary result related to the structure of $S_{(r,g)}$. In the following lemma, we show that the success rate at a given (r,g) is decreasing in g and increasing r; also, it rises if the g falls maximally as r falls.

Lemma 1 (Success rate). *The success rate $S_{(r,g)}$ satisfies the following properties:*

i threshold effect: For any fixed $r \in \{0,T\}, S_{(r,g)} \leq S_{(r,g-1)}$;

ii bad-news (duration) effect: For any $g \in \{K-T,K\}, S_{(r-1,g)} \leq S_{(r,g)}$;

iii good-news effect: for any $g \in \{K-T,K\}$, $S_{(r-1,g-1)} \geq S_{(r,g)}$.

Proof of Lemma 1. In Appendix C ■

Part (i) is intuitive: a lower gap implies a higher chance of success because fewer bids are required to reach the funding goal. Such effect occurs at a campaign design stage by setting a lower threshold. Part (ii) comes from the observation that having less time to fill the gap reduces the probability of success. While the campaign is started, observing that r reduces by one at a fixed g carries the bad news that there was no bid at r. At the design stage this effect is produced by setting lower duration. For part (iii), note that the success rate necessarily

[8] Assuming multiple arrivals the game can have a multiple equilibria due to possible coordination failure.

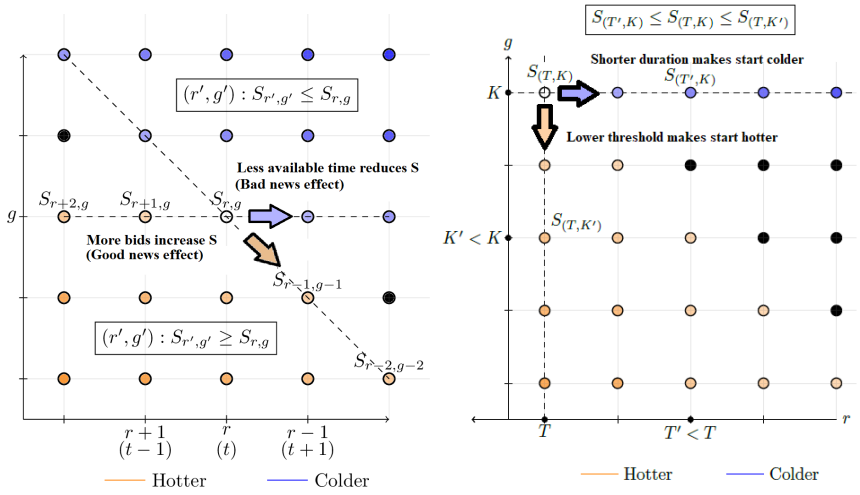

Figure 1: Monotonicity of $S_{(r,g)}$ in the $(g, t = T - r + 1)$ space

increases when the best bidding outcome arises in a given time interval. This is a good-news effect that is produced within campaign. [9]

3.2 Bid profiles

In this section we analyse the general properties of bidding profiles. We start by presenting the following general rules. If $T = K$, there is only one possible path to success: a bid in every period. So conditioning on success, the bid profile is flat at unity: $A_r^{\mathcal{S}} = 1$ for all r. Also, if $K = 1$, then clearly $A_r^{\mathcal{F}} = 0$ for all r. No threshold always implies a flat profile.If $K > T$, then the campaign can never succeed, so bidding only comes from bidders with negative or null inspection cost, and $A^{\mathcal{S}}$ is undefined.

In general, the slope of the bid profile varies over time. To calculate expected change in bids across two consecutive periods, r and $r-1$, suppose only one bid arises at r or $r-1$. We want to understand when it is more likely to occur sooner than later. The two possible paths the gap can follow correspond to the dashed and dotted lines between nodes (r, g) and $(r-2, g-1)$ presented in Fig. 1. The high road has no bid at r with probability $1 - p_{(r,g)}$ followed by a bid lowering g to $g-1$ at $r-1$ with probability $p_{(r-1,g)}$, so the high road (or *delayed bid* path) occurs with probability $(1 - p_{(r,g)})p_{(r-1,g)}$. The low road has a bid at r with probability $p_{(r,g)}$, lowering the gap form g to $g-1$, and no bid at $r-1$, with probability $1 - p_{(r-1,g-1)}$. Thus the low road (or *early bid* path) is followed with probability $p_{(r,g)}(1 - p_{(r-1,g-1)})$. Note that if two or no bids are collected the resulting profile is flat, so we can focus on the cases considered. Moreover, since the transition probabilities across nodes are governed by a Markovian process, what happens between (r, g) and $(r-2, g-1)$ is independent of the path from (T, K) to (r, g), and from (r, g) to the final nodes. Therefore, the expected change in bids, $A_{r-1} - A_r$ is identical to the expectation of

$$\Delta_{(r,g)} = (1 - p_{(r,g)})p_{(r-1,g)} - p_{(r,g)}(1 - p_{(r-1,g-1)}) \tag{16}$$

[9] Part (iii) of lemma 1 does not hold if we assume multiple arrivals or endogenous movers.

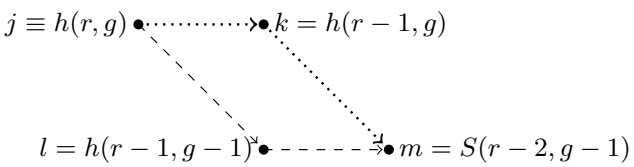

Figure 2: Heat on the early and delayed paths

with respect to g. Similarly, the expected change in bids of successful (failed) campaigns in two consecutive periods is the expectation of $\Delta_{(r,g)}$ conditional on a success (failure) in reaching the threshold by period $r = 0$ after collecting only one bid among periods r and $r-1$. Formally, letting

$$\begin{aligned} \Delta^{\mathcal{S}}_{(r,g)} &\triangleq \Delta_{(r,g)} S_{(r-2,g-1)} \\ \Delta^{\mathcal{F}}_{(r,g)} &\triangleq \Delta_{(r,g)} \left(1 - S_{(r-2,g-1)}\right) \end{aligned} \tag{17}$$

We can also see that the variation in bid rates from any given node is determined by the change in heat along paths that cross the rhombus in figure Fig. 2, and amplified (weakened) by the interim probability of success for successful (failed) campaigns.

the following lemma summarizes how to represent the difference in consecutive period bids in terms of $\Delta_{(r,g)}$.

Lemma 2 (Expected change in consecutive bids)**.** *The expected change in bids is given by*

$$\begin{aligned} A_{r-1} - A_r = \mathbb{E}_g\left[\Delta_{(r,g)}\right] &\equiv \sum_{g=K-(T-r)}^{K} P_{(r,g)} \Delta_{(r,g)} \\ A^{\mathcal{S}}_{r-1} - A^{\mathcal{S}}_r = \mathbb{E}_g\left[\Delta_{(r,g)} \mid \mathcal{S}\right] &\equiv \frac{1}{S} \sum_{g=K-(T-r)}^{K} P_{(r,g)} \Delta^{\mathcal{S}}_{(r,g)} \\ A^{\mathcal{F}}_{r-1} - A^{\mathcal{F}}_r = \mathbb{E}_g\left[\Delta_{(r,g)} \mid \mathcal{F}\right] &\equiv \frac{1}{1-S} \sum_{g=K-(T-r)}^{K} P_{(r,g)} \Delta^{\mathcal{F}}_{(r,g)} \end{aligned} \tag{18}$$

Proof of Lemma 2. In Appendix C. ■

A direct consequence Lemma 2 is that, if the delayed bid path is always more likely than the early bid path, then bidding profile rises over time. If the opposite holds, then the profile falls over time.[10]

Corollary 1. *If $\Delta_{(r,g)} \geq 0$ for all (r,g), the aggregate bid profile is increasing over time. Similarly, if $\Delta^{\mathcal{S}}_{(r,g)} \geq 0$ ($\Delta^{\mathcal{F}}_{(r,g)} \geq 0$) for all (r,g) the S-profile (F-profile) is increasing over time. If the opposite of any previous condition hold, then the profile it refers to decreases over time.*

In the remaining part of the current section, we solve algorithmically the model under different cost distributions and use Lemma 2 and Corollary 1 to determine the properties of the bid profile.

[10] Increasing over time means decreasing in r.

3.3 Homogeneous inspection costs

In the setting where all bidders have the same inspection cost c, the campaign has two possible heat levels: hot or frozen. At hot nodes, all bidders choose C and at frozen nodes, they all choose A. That is, at hot nodes $(r, g) \in H$, bidders inspect and the campaign receives an additional bid with probability λq. Conversely, at frozen nodes, $(r, g) \in F$, bidders abstain.

$$p_{(r,g)} = \begin{cases} \lambda q & \text{if } (r, g) \in H \\ 0 & \text{if } (r, g) \in F \end{cases} \tag{19}$$

We call the heat contour that separates the two regions, the "wall of ice," since gap g becomes frozen at $g = g_r$ if the (r, g) path hits this countour at rem r. The contour of wall is mapped out by the points $(r, \hat{g}_{(r)})$ with r falling from T to 1 and $\hat{g}_{(r)}$ representing the highest (integer) gap at which bidders would choose C given rem r. Instead of working with the vector of gap thresholds $\hat{\boldsymbol{g}}_{=}(\hat{g}_{(1)}, \hat{g}_{(2)}, \cdots, \hat{g}_{(T)})$, one can use the vector of rem thresholds $\hat{\boldsymbol{r}} = (\hat{r}_{(1)}, \hat{r}_{(2)}, \ldots, \hat{r}_{(K)})$ which indicate the highest rem at which bidders are willing to choose C given that $g \geq 1$. We adopt the convention that $\hat{g}_{(r)} = +\infty$ if bidder r chooses C for all g, and $\hat{g}_{(r)} = -\infty$ if he chooses A for all g. Similarly, we let $\hat{r}_{(g)} = 0$ if bidders observing gap g would inspect at any rem and $\hat{r}_{(g)} = +\infty$ for a gap that dissuades choice C no matter how much time remains. So, letting $G = \{0, \ldots, K\}$,

$$\hat{g}_{(r)} \triangleq \max\{g \in G \cup \{-\infty, +\infty\} \mid \hat{c}_{(r,g)} \geq c\} \tag{20}$$

$$\hat{r}_{(g)} \triangleq \min\{r \in \{0, 1, \ldots, T\} \cup \{+\infty\} \mid \hat{g}_{(r)} \geq g\} \tag{21}$$

Where $\hat{c}_{(r,g)}$, defined in Eq. (13), is the value of $c_{r,g}$ that makes bidders indifferent between A and C. We define $\tilde{g}_{(r)}$ and $\tilde{r}_{(g)}$ as the solutions to[11]

$$\tilde{g}_{(r)} \triangleq g \in \mathbb{R} \cup \{-\infty, +\infty\} : qS_{(r-1,g-1)} = c \tag{22}$$

$$\tilde{g}_{(r)} \triangleq r \in \mathbb{R}_+ \cup \{+\infty\} : qS_{(r-1,g-1)} = c \tag{23}$$

If Eq. (22) has no solution, we say that $\tilde{g}_{(r)}$ does not exist. Whenever it does exist, $\hat{g}_{(r)}$ is the greatest integer less than or equal to $\tilde{g}_{(r)}$, so $\lfloor \tilde{g}_{(r)} \rfloor = \hat{g}_{(r)}$.

When reaching a node puts the campaign in a permanent hot state we say that the campaign is boiling. This occurs at nodes where $S_{(r-1,g-1)} = 1$, thus at any node (r, g) with $g \leq 1$. The following lemma describes the basic properties of the ice frontier.

Lemma 3 (Heat contours)**.** *The ice frontier* $\hat{\boldsymbol{g}} = (\hat{g}_{(1)}\ \hat{g}_{(2)}\ \cdots\ \hat{g}_{(T)})$ *satisfies the following properties:*

i $\hat{g}_{(r)}$ *is increasing in* r

ii $\hat{g}_{(r)} - \hat{g}_{(r-1)} \leq 1$

iii $S_{(r,g|\hat{\boldsymbol{g}}_{\boldsymbol{r-1}})} \geq S_{(r,g|\hat{\boldsymbol{g}}'_{\boldsymbol{(r-1)}})}$ *for all* $\hat{\boldsymbol{g}}_{\boldsymbol{r-1}} \geq \hat{\boldsymbol{g}}'_{\boldsymbol{(r-1)}}$

[11] The solution for g is generically not an integer, but we use the Beta function as continuous extension of all the binomial terms, from integer g to the full real line.

iv $\hat{\boldsymbol{g}}(c') \leq \hat{\boldsymbol{g}}(c)$ *for all* $c' > c$.[12]

Proof of Lemma 3. In Appendix C ■

The direct consequence of Lemma 3 is that the ice frontier is decreasing in time and makes at most a unit step between subsequent values. Formally,

$$0 \leq g_r - g_{r-1} \leq 1 \iff g_{r-1} \in \{g_r, g_r - 1\} \tag{24}$$

Figure Appendix D shows a sucessful and a failed simulated path and bids.

Figure 3: The ice frontier

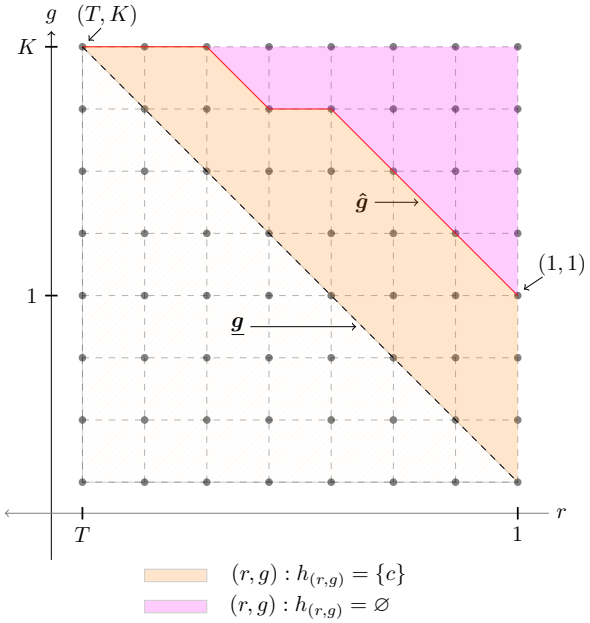

The fact that the campaign can only pass from hot to frozen makes the aggregate bid profile decreasing. To see this, note that the campaign can only change heat once passing from hot to frozen. As shown in figure Fig. 4, it stays hot for $g < \hat{g}_{(r)}$ and frozen for $g > \hat{g}_{(r)}$. We let

$$\pi_r \triangleq \mathbb{P}\left(g_r \leq \hat{g}_{(r)}\right) \tag{25}$$

denote the probability that the campaign is hot. At $\hat{g}_{(r)}$, it can the frozen if the wall drops, i.e. for $\hat{g}_{(r)} = \hat{g}_{(r-1)} + 1$. At such node the expected change in the aggregate bid rate is negative and equal to $\Delta_{(r,\hat{g}_{(r-1)}+1)} = -\lambda q(1 - \lambda q)$. Conversely if $\hat{g}_{(r)} = \hat{g}_{(r-1)}$, the campaign stays hot. The possibility of crossing the ice frontier generates a time-increasing freezing rate that makes the profile decreasing.

Lemma 4. *(Freezing rate) If* $c_r = c$ *for all* r*, the aggregate profile gradually decreases due to a time-increasing freezing rate.*

Proof of Lemma 4. In Appendix C ■

Indeed, we can further prove that also the conditional profiles are decreasing using Corollary 1. Intuitively, a decreasing pattern arises for successful campaigns due to the prevalence of

[12] $\hat{\boldsymbol{g}} \geq \hat{\boldsymbol{g}}'_{()}$ is equivalent to $\hat{g}_{(r)} \geq \hat{g}'_{(r)}$ for all r and there is at least one r such that $\hat{g}_{(r)} > \hat{g}'_{(r)}$.

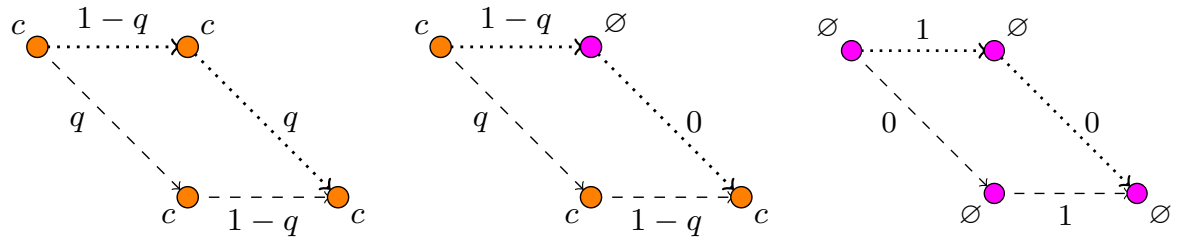

(i) $\Delta_{(r,g)} = 0$ (ii) $\Delta_{(r,g)} = -\lambda q(1-\lambda q)$ (iii) $\Delta_{(r,g)} = 0$

Figure 4: (i) $g < \hat{g}_{(r)}$ or $g = \hat{g}_{(r)}, \hat{g}_{(r)} = \hat{g}_{(r-1)}$, (ii) $g > \hat{g}_{(r)}$, (iii) $g = \hat{g}_{(r)}, \hat{g}_{(r)} = \hat{g}_{(r-1)} + 1$

early bidding among success, keeping the gap far from the ice frontier. For failed campaign instead the bid rate decreases for the same freezing probability motive we saw for the unconditional case.

Proposition 2. *If $c_r = c$ for all r, the aggregate and conditional profiles are decreasing over time.*

Proof of Proposition 2. In Appendix C ■

To illustrate the fundamental properties of the profile when bidders arrivals are frequent, we study the continuous-time limit of the model. A technical derivation is provided in Appendix A. We consider a campaign of goal $K = 2$ and duration τ made of infinitesimally small periods. Observing $g = 2$, bidders are willing to inspect for $r \geq \hat{r}_{(2)}$, defined as

$$\hat{r}_{(2)} \triangleq r \geq 0 : qS_{(\hat{r}_{(2)},1)} = c \tag{26}$$

Using D as the derivative with respect to r, Eq. (70) implies that $D(log(1-S_{(r,1)})) = -\lambda q \, \forall r \geq 0$. It follows at once that,

$$S_{(r,1)} = 1 - Q_{(r,1;0,1)} = 1 - e^{-\lambda q r} \tag{27}$$

hence

$$S_{(\hat{r}_{(2)},1)} = 1 - e^{-\lambda q \hat{r}_{(2)}}$$

so $\hat{r}_{(2)}$ is given by

$$\hat{r}_{(2)} = \frac{1}{\lambda q} \ln\left(1 - \frac{c}{q}\right)^{-1} \tag{28}$$

Notice that it is strictly positive, increasing in c and decreasing in λ. To apply the methodology presented in Appendix A to compute the aggregate and conditional expected intensities of bidding at rem r, we need to compute the bid intensities $p_{(r,2)}$ and $pr, 1$; the probability of no bids collected by rem r, $P_{(r,2)}$; the ex-ante success rate S, and the after-pledging success rate $S'_{(r,2)} = S_{(r,1)}$. First, bidding intensities at a given node are $p_{(r,1)} = p_{(r,2)} = \lambda q$ for $r \geq \hat{r}_{(2)}$ and $p_{(r,1)} = \lambda q$ $p_{(r,2)} = 0$ otherwise. As a consequence, if the campaign is frozen at start bidding is null. This requires $\tau \geq \hat{r}_{(2)}$ to have some bidding. In this case the campaign carries a risk of freezing at $\hat{r}_{(2)}$ if the gap is not unity. We can see that the probability that the campaign gets

Figure 5: Bid, gap profiles and ice frontier with homogeneous inspection cost

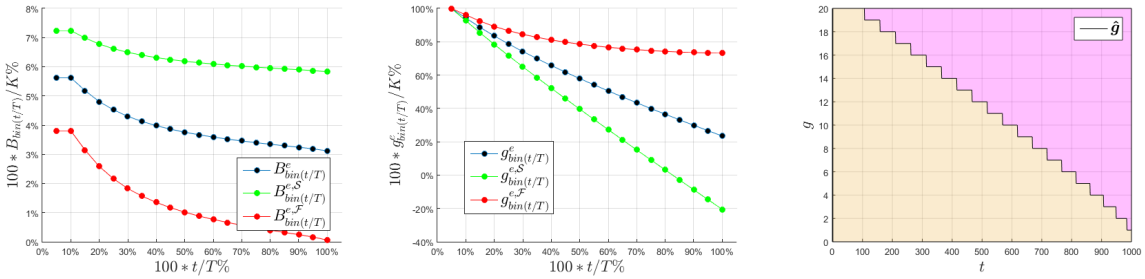

Parameters $T = 50n$, $K = 20$, $q = .5$, $c = .15$, $\lambda = .9/n$, $n = 20$

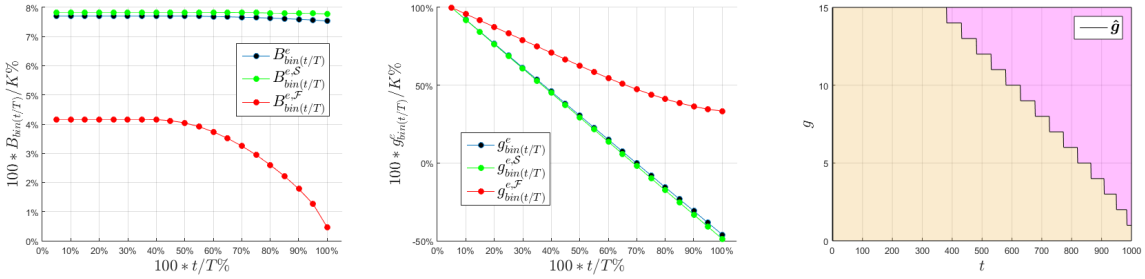

Parameters $T = 50n$, $K = 15$, $q = .5$, $c = .15$, $\lambda = .925/n$, $n = 20$

Bid rates and expected gaps are aggregated at each 5% of campaign's duration. $B^e(t/T)$ is the bid rate for bin t/T. Expected gaps and bids in each bin are expressed relative to the funding goal K, while time is relative to the duration T. Bid rates are presented in Fig. 13

frozen is given by

$$\begin{aligned} P_{(\hat{r}_{(2)},2)} &= e^{-\lambda q(\tau-\hat{r}_{(2)})} \\ &= \left(1-\frac{c}{q}\right)^{-1} e^{-\lambda q\tau} \end{aligned}$$

consequently,

$$P_{(r,2)} = \begin{cases} e^{-\lambda q(\tau-r)} & \text{for } r \geq \frac{1}{\lambda q}\ln\left(1-\frac{c}{q}\right)^{-1} \\ \left(1-\frac{c}{q}\right)^{-1} e^{-\lambda q\tau} & \text{for } r < \frac{1}{\lambda q}\ln\left(1-\frac{c}{q}\right)^{-1} \end{cases} \tag{29}$$

The ex-ante success rate is the probability of collecting two bids where at least one lays in the initial hot region. So

$$\begin{aligned} S &= 1 - \left(P_{(\hat{r}_{(2)},2)} + P_{(\hat{r}_{(2)},1)} Q_{(\hat{r}_{(2)},1;0,1)}\right) \\ &= 1 - \left(e^{-\lambda q(\tau-\hat{r}_{(2)})} + \int_{r=\hat{r}_{(2)}}^{\tau} e^{-\lambda q(\tau-r)} \lambda q e^{-\lambda q r}\right) \\ &= 1 - e^{-\lambda q\tau}\left[\left(1-\frac{c}{q}\right)^{-1} + \lambda q\tau - \ln\left(1-\frac{c}{q}\right)^{-1}\right] \end{aligned}$$

for $\tau \geq \hat{r}_{(2)}$ and 0 otherwise. The Aggregate and conditional bid rates are given by

$$A_r = \begin{cases} \lambda q & \text{for } r \geq \frac{1}{\lambda q} \ln\left(1-\frac{c}{q}\right)^{-1} \\ \lambda q\left(1-\left(1-\frac{c}{q}\right)^{-1} e^{-\lambda q \tau}\right) & \text{for } r < \frac{1}{\lambda q} \ln\left(1-\frac{c}{q}\right)^{-1} \end{cases} \tag{30}$$

$$A_r^{\mathcal{S}} = \begin{cases} \frac{1}{S}\lambda q\left(1-e^{-\lambda q r}\right) & \text{for } r \geq \frac{1}{\lambda q} \ln\left(1-\frac{c}{q}\right)^{-1} \\ \frac{1}{S}\left(1-\left(1-\frac{c}{q}\right)^{-1} e^{-\lambda q \tau}\right)\lambda q & \text{for } r < \frac{1}{\lambda q} \ln\left(1-\frac{c}{q}\right)^{-1} \end{cases} \tag{31}$$

$$A_r^{\mathcal{F}} = \begin{cases} \frac{1}{1-S}\lambda q e^{-\lambda q \tau} & \text{for } r \geq \frac{1}{\lambda q} \ln\left(1-\frac{c}{q}\right)^{-1} \\ 0 & \text{for } r < \frac{1}{\lambda q} \ln\left(1-\frac{c}{q}\right)^{-1} \end{cases} \tag{32}$$

From the previous expression we can see that A_r is flat at λq at start and then drops and is flat at qpi_r, from $\hat{r}_{(2)}$, where $\pi_r = 1 - e^{-\lambda q(\tau - \hat{r}_{(2)})}$. $A_r^{\mathcal{S}}$ shows an initially time decreasing profile for then becoming flat after $\hat{r}_{(2)}$. The initial effect is do to the prevalence of early bids among successes. Failed campaigns are initially constant as the moment the bid is collected does not affect the chances of being on a failing path where that is the only bid collected. At $\hat{r}_{(2)}$ the intensity drops at 0 because, if no bid is collected, the campaign is frozen and if one bid is collected a failed campaign cannot collect more. The following lemma summarizes these findings:

Lemma 5. *homogeneous cost, $K = 2$, continuous time In continuous time and for $K = 2$ campaigns, the bid profile is discontinuous, decreasing on aggregate and for successful campaigns and non-monotone for failed campaigns, first constant and then null.*

3.4 Binary inspection costs

In this section we assume that inspection costs binary; that is, each bidder's inspection cost is either c_L or c_H with probability z on c_L.[13]

The states of heat are either frozen, cold or hot.

$$p_{(r,g)} = \begin{cases} \lambda q & \text{if } h(r,g) = H \\ \lambda z q & \text{if } h(r,g) = L \\ 0 & \text{if } h(r,g) = 0 \end{cases} \tag{33}$$

For $c_L = 0$, $c_H \equiv c > 0$ there are two states: $j = L$ or H. $j = 0$ never occurs because L-types enjoy inspecting and do so every time they arrive. The bid rate is affected by whether H-types are also willing to play C or instead play A. We say that the project is hot if H-types play C and cold if they play A. [14] Similarly to the setting presented in Section 3.3, the two states

[13] If $c_L = c_H$, the analysis is equivalent to the case of homogeneous inspection costs.

[14] If guaranteed failure, L-types might inspect and then not bid, but we assume bid when indifferent to ensure congruence with the continuous time scenario in which there is almost always time to reach any given gap so

are separated by the heat contour $\hat{\boldsymbol{g}} = (\hat{g}_1, \hat{g}_2, \ldots, \hat{g}_T)$ which satisfies the properties stated in Lemma 3.

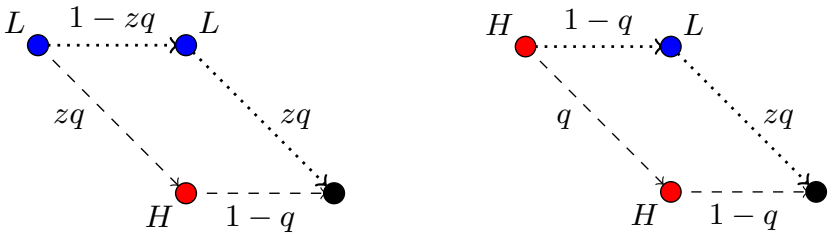

(i) $\Delta_{(r,g)} = (\lambda q)^2 z(1-z) > 0$ (ii) $\Delta_{(r,g)} = -\lambda q(1-z)(1-\lambda q) < 0$

Figure 6: $\Delta_{(r,g)}$ at nodes where a change of heat can take place.

We can see that $\Delta_{(r,g)} = 0$ unless heats at the vertices of the rhombus in Fig. 2 are $(k, m, .; j) = (L, H, .; L)$ or $(L, H, .; H)$. The former path implies $\Delta_{(r,g)} > 0$ while latter implies $\Delta_{(r,g)} < 0$. The first case occurs at a node where the frontier can be crossed from the cold region, for $\hat{g}_{(r-1)} = \hat{g}_{(r)}$ and $g_r = \hat{g}_{(r)} + 1$; the latter at nodes where it can be crossed from the hot region, for $\hat{g}_{(r-1)} = \hat{g}_{(r)} - 1$ and $g_r = \hat{g}_{(r)}$. The reason for these signs is that the delayed path in former has no-bid at $j = L$ while both early and late have the bid at $l = L$; Conversely, early path has bid in hot $j = H$ while delayed path has the bid in cold $j = L$ state. Formally,

$$\Delta_{(r,\hat{g}_{(r)}+1)} = (1-\lambda zq)\lambda zq - \lambda zq(1-\lambda q) = (\lambda q)^2 z(1-z) > 0 \text{ for } \hat{g}_{(r-1)} = \hat{g}_{(r)}$$
$$\Delta_{(r,\hat{g}_{(r)})} = (1-\lambda q)\lambda zq - \lambda q(1-\lambda q) = -\lambda q(1-z)(1-\lambda q) < 0 \text{ for } \hat{g}_{(r-1)} = \hat{g}_{(r)} - 1$$

We find that the profile can be increasing if the campaign starts cold and the heat contour is sufficiently convex. This makes it easier to have heats on transition paths of $(LL; H.)$ than $(HL; H)$. To avoid possible non-monotonicities we need a cold start that leads gradually to a permanent hot state. This can be achieved only when reaching the frontier makes the campaign boiling; that is, when it can be reached only at a unitary gap. The condition

$$c > \underline{c}_H \triangleq q\left(1 - (1-\lambda q)^{T-K+1}\right) \tag{34}$$

ensures so. When it holds, if wall is above unity, it cannot be reached at the lowest achievable gap of $K - T + r$. We can also obtain a decreasing profile when the campaign starts hot and moves to a permanent cold states; e.g. when they imply a success rate of 0. This occurs for

$$c \leq \overline{c}_H \triangleq \frac{(\lambda q)^K}{\lambda} \tag{35}$$

For intermediate values of c, the profile is non-monotonic due to possible in-and-out from the two heat regions. However, when bidders arrive in continuous time and the arrival rate is sufficiently low, the increasing region top the cold and non-monotone becoming the dominant effect.

The following proposition summarizes our findings for Section 3.4

that with $c_L = 0$, the success rate may be arbitrarily close to 0 but never equals zero.

Figure 7: Expected gap, bid rate and cold frontier. Bid rates are presented in Fig. 14.

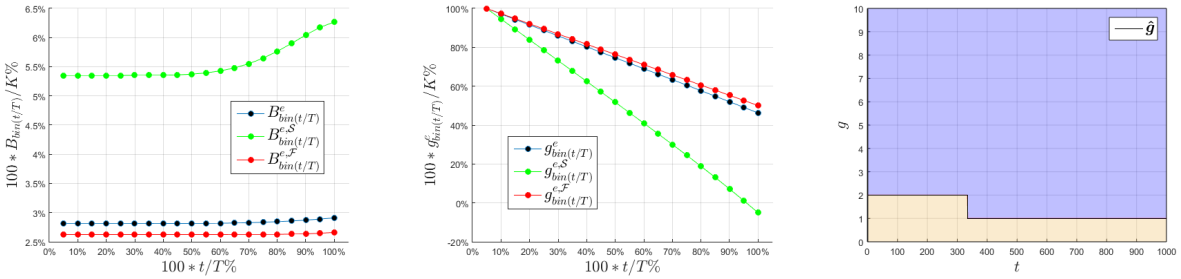

$(T = 20n,\ K = 10,\ q = .75,\ z = .75,\ c_H = 745,\ \lambda = .5/n,\ n = 50)$

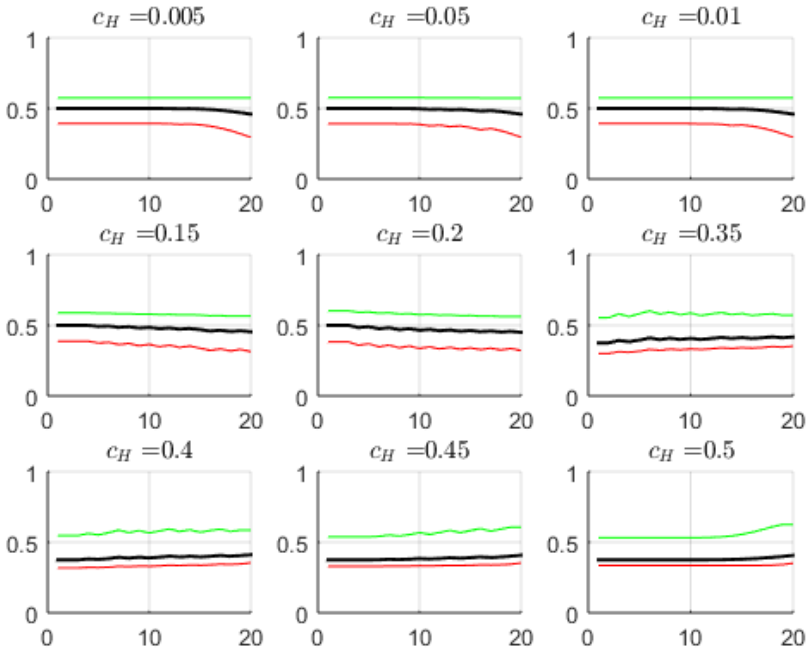

Figure 8: Bid profiles. $c_L = 0$, c_H from .005 to .05. $()T = 20$, $K = 10$, $q = .5$, $c_L = 0$)

Proposition 3. *When $c_L \leq 0$ and $c_H > 0$, the profile is decreasing for $c_H \in \left[0, \frac{(\lambda q)^K}{\lambda}\right]$, increasing for $c_H \in \left(q\left(1-(1-\lambda q)^{T-K+1}\right), q\right]$, and non-monotone in the middle region. Moreover, aggregate and conditional bid profiles change slope in the same direction.*

Proof of Proposition 3. In Appendix C ■

We again use the continuous time model to corroborate the findings obtained and provide an example of increasing bid profile under cold start for $K = 2$. Similarly to Section 3.3, there exist an $\hat{r}_{(2)}$ that determines a shift from hot to cold state when $g = 2$, which is again determined by Eq. (28) by replacing setting $c = c_H$. In this example, the campaign remains cold until the first bid is collected. At that time, it enters a boiling state and stays hot until its end. We have a "cold start" for $\tau < \hat{r}_{(2)}$. Bidding intensities are $p_{(r,1)} = \lambda q$, $p_{(r,2)} = \lambda z q$ for $r \geq \hat{r}_{(2)}$ and $p_{(r,2)} = \lambda q$ for $r < \hat{r}_{(2)}$. We now compute the other quantities required to pin-down the time intensity of bidding. Under cold start, the probability that the campaign is cold at r is $P_{(r,2)}$;

that is,

$$P_{(r,2)} = e^{-\lambda zq(\tau - r)} \tag{36}$$

The ex-ante success rate is given by

$$S = 1 - \left(P_{(0,2)} + P_{(0,1)}\right)$$

$P_{(0,2)} = e^{-\lambda zq\tau}$ is the probability that no bid is collected at all. $P_{(0,1)}$ is instead the probability of collecting only one bid. We obtain $Q_{(r,2;0,1)}$ by integrating out s, the moment the first bid occurs, from the probability of collecting no bid after then, $Q_{(s,1;0,1)} = e^{-\lambda qs}$. Since the time density of s is $P_{(s,2)}zq = e^{-\lambda zq(\tau - s)}zq$ we find that

$$\begin{aligned} Q_{(r,2;0,1)} &= \int_0^\tau P_{(s,2)}(\lambda qz)Q_{(s,1;0,1)}ds \\ &= \int_0^\tau e^{-\lambda zq(\tau - s)}\lambda qz e^{-\lambda qs}ds \\ &= \frac{z}{1-z}\left(e^{-\lambda zq\tau} - e^{-\lambda q\tau}\right) \end{aligned}$$

adding up the two terms previously computed, we find that

$$S = 1 - \frac{e^{-\lambda zq\tau} - ze^{-\lambda q\tau}}{1-z} \tag{37}$$

Thus using Eqs. (72) to (74), we find that aggregate and conditional bid intensities at rem r are given by [15]

$$A_r = \lambda q\left(1 - \underbrace{e^{-\lambda zq(\tau - r)}}_{1-\pi_r}(1-z)\right) \tag{38}$$

$$A_r^{\mathcal{S}} = \frac{1}{S}\lambda q\left[1 - \underbrace{e^{-\lambda zq(\tau - r)}}_{1-\pi_r}\left(1 - z\underbrace{\left(1 - e^{-\lambda qr}\right)}_{S_{(r,1)}}\right)\right] \tag{39}$$

$$A_r^{\mathcal{F}} = \frac{1}{1-S}\left[\underbrace{e^{-\lambda qz(\tau - r)}}_{1-\pi_r}(\lambda qz)\ \underbrace{e^{-\lambda qr}}_{1-S_{(r,1)}}\right] \tag{40}$$

Evidently, A_r is time-increasing owing to the heating effect cause by L-types. Conversely, the slope of $A_r^{\mathcal{S}}$ is the result of two contrasting effects of time; that is, when more time is available, bidding intensities are reduced by the lower chances that the campaign is hot but also raised by the prevalence of early bidding to successful campaigns. The prevailing effect determines whether the profile shows a tendency towards delayed or early bidding. Formally, since $\dot{F}\left(\hat{c}_{(r,g)}\right) = 0$, we use Eq. (79) to find that $\dot{A}_r^{\mathcal{S}}$ is proportional to $e^{-\lambda qr} + z\left(1 - e^{\lambda qr}\right) - 1 < 0$. For failed campaigns, the effect of time is clearly the opposite since this last force has the opposite effect; that is, early bids are less prevalent among failed campaigns as the make the failure rate particularly low.

[15] Even if not explicit, in equation Eq. (39) bidding at $g = 1$ produces success, so the bid rate of successful campaigns at nodes $(r, 1)$ is simply $\lambda q S_{(r,0)} = \lambda q$.

Hence failed campaign are clearly increasing in time. Note also that as a result of the shift caused by conditioning on outcome, in this example, the S-profileis concave in time while the F-profileis convex.

For $\tau < \hat{r}_{(2)}$, have have a "hot start". Analogously to what we saw in Section 3.3, heat and bid profiles drop discontinuously at $\hat{r}_{(2)}$. The campaign can either (i) remain hot until the end; (ii) get cold and remain as such; or (iii) get cold and return hot before ending. We clearly have

$$P_{(r,2)} = \begin{cases} e^{-\lambda q(\tau - r)} & \text{for } r \geq \frac{1}{\lambda q}\left[\ln\left(1 - \frac{c_H}{q}\right)^{-1}\right] \\ e^{-\lambda q(\tau - zr)}\left(\frac{q}{q - c_H}\right)^{1-z} & \text{for } r < \frac{1}{\lambda q}\left[\ln\left(1 - \frac{c_H}{q}\right)^{-1}\right] \end{cases} \tag{41}$$

To compute conditional profiles, we first need to determine S. To do so we take the complement of the fail rate; e.g. the probability that it either collects no or one bid. The second event takes place when only one bid is collected at a given rem s. Formally,

$$\begin{aligned} S &= 1 - \left[P_{(\hat{r}_{(2)},2)} Q_{(\hat{r}_{(2)},2;0,2)} + \left(P_{(\hat{r}_{(2)},1)} Q_{(\hat{r}_{(2)},1;0,1)} + P_{(\hat{r}_{(2)},2)} Q_{(\hat{r}_{(2)},2;0,1)}\right)\right] \\ &= 1 - \left[e^{-\lambda q(\tau - \hat{r}_{(2)}) - \lambda q z \hat{r}_{(2)}} + \left(\lambda q(\tau - \hat{r}_{(2)}) e^{-\lambda q \tau} + e^{-\lambda q(\tau - \hat{r}_{(2)})} \int_0^{\hat{r}_{(2)}} e^{-\lambda z q(\hat{r}_{(2)} - s)} \lambda z q e^{-\lambda q s} ds\right)\right] \\ &= 1 - e^{-\lambda q \tau}\left\{\left(1 - \frac{c_H}{q}\right)^{-1} + \lambda q \tau - \ln\left(1 - \frac{c_H}{q}\right)^{-1} - \frac{z}{1-z}\left[1 - \left(1 - \frac{c_H}{q}\right)^{z-1}\right]\right\} \end{aligned} \tag{42}$$

For $z = 0$ this expression coincides with Eq. (30). For $z \to 1$ we get close to a scenario where we have only one cost-type bidder with $c_H = c_L = 0$. Applying L'Hôpital's rule to find that $\lim_{z\to 1} \frac{z}{1-z}\left[1 - \left(1 - \frac{c_H}{q}\right)^{z-1}\right] = \ln\left(1 - \frac{c_H}{q}\right)$ and letting $c_H \to 0$ we find that

$$S = 1 - e^{-\lambda q \tau}(1 + \lambda q \tau) \tag{43}$$

It can be verified using Eq. (69) that this is the probability of collecting one or no bid for $F(0) = 1$; that is, when all bidders have no inspection cost.

The aggregate bid intensity is given by

$$A_r = \begin{cases} \lambda q & \text{for } r \geq \frac{1}{\lambda q}\ln\left(1 - \frac{c_H}{q}\right)^{-1} \\ \lambda q\left[1 - e^{-\lambda q(\tau - r)}\left(1 - \frac{c}{q}\right)^{z-1}(1 - z)\right] & \text{for } r < \frac{1}{\lambda q}\ln\left(1 - \frac{c_H}{q}\right)^{-1} \end{cases} \tag{44}$$

We can easily see from Eq. (44) that the profile is initially constant, drops at $\hat{r}_{(2)}$ and is increasing over time afterwards. In some sense, it can be fall into the category of "U-shapes". Conditional profiles present similar features and are presented in Appendix B. The following lemma summarizes the analysis developed so far on continuous time with binary inspection costs.

Lemma 6 (Cold and Hot start for $K = 2$ campaigns)**.** *In continuous time, the bid profile of $K = 2$ campaigns is increasing under cold start and discontinuous under hot start. In particular, the aggregate profile under hot start is "U-shaped".*

Figure 9: Expected gap and bids for uniform distribution. Bid rates in Fig. 15

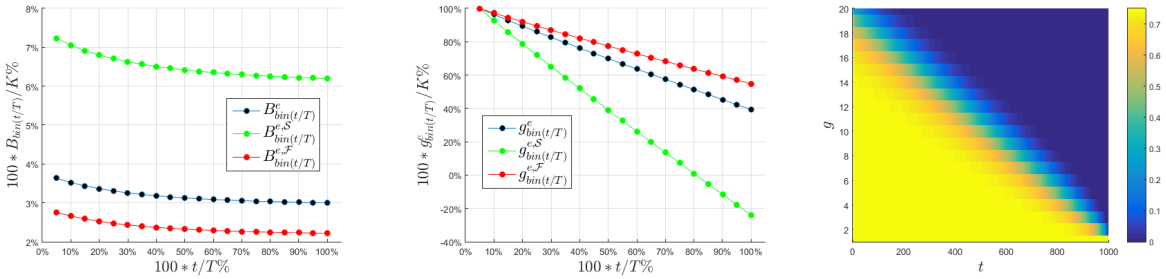

Parameters: $T = 20n$, $K = 20$, $q = .75$, $z = .25$, $f = .75$, $\lambda = .95/n$, $n = 50$

The next section is devoted to the study of distributions with a continuum of inspection cost. We answer the question of what profile generates a uniform distribution with an atom of positive mass at $c = 0$.

3.5 Uniform distribution with atom at 0

We consider now the case where c_r's is 0 with probability $z < 1$ and is uniformly distributed with mass f over $[0, 1/f]$ for $f \leq 1/q$ with probability $1 - z$.[16]. Key difference with the binary setting is that there is a continuum of heat states given by $h_{(r,g)} = \hat{c}_{(r,g)}$. In this setting, $F(c) = z + (1 - z)fc$ for $c \in [0, 1/f]$, $F(c) = 1$ for $c \geq 1/f$, $F(c) = z$ for $c \leq 0$. The conditional bid rate is given by

$$p_{(r,g)} = \lambda q[z + (1 - z)f \min\{qS_{(r-1,g-1)}, 1/f\}] \tag{45}$$

Using proposition 1, we can easily see that the bidding profile is downward sloping.[17] To understand why, note that $p_{(r,g)}$ is linear in $S' = S_{(r-1,g-1)}$ and by the martingale property of S (and therefore S'), is also a sub-martingale. If $p_{(r,g)}$ were linear in $S_{(r,g)}$, then by the martingale property it would lead to a flat (neutral) aggregate profile. However, bidders evaluate the decision to inspect under the optimistic view of liking the good and contributing. This generates linearity in $S_{(r-1,g-1)}$. On the other hand, the expectation of next period bids involves less optimism since unconditional on good news. This delivers a lower expectation of future bids and implies an expected decline in the bid rate. This good-news effect is larger the more bidder r is *pivotal*. A higher pivotality early on as a result of good news on future bidders and a higher impact of news when little information is revealed during at the proximity of the starting date would suggest that the profile is convex.[18].

Proposition 4 (Dynamic profile under uniformly distributed inspection costs with atom at 0)**.** *If c_r is 0 with probability z and uniformly distributed with mass f over $[0, 1/f]$ with probability $1 - z$, then the bid profile is decreasing.*

[16] An atom at 0 produces the same effect on bidding profiles as a positive mass on negative inspection costs. If c follows a uniform distribution on $[\underline{c}, \overline{c}]$ with $\underline{c} < 0$, then $F(c) = \underline{c}/(\underline{c} + \overline{c}) + \min\{c, \overline{c}\}/(\overline{c} + \underline{c})$ for $c \geq 0$. By letting $z = \underline{c}/(\underline{c} + \overline{c})$ and $f = 1/\overline{c}$ we obtain the same distribution.

[17] Result might be affected by a lower bound above 0.

[18] Clearly if K is huge, then S is near 0 and the effect of pivotality is small. Note also that close to end pivotality can be huge but on average tends to be small.

Proof of Proposition 4. In Appendix C. ■

Again using the continuous model we obtain the same slope prediction than the discrete one. Consider the continuous model with $K = 2$ and $f = \frac{1}{q}$, so that the distribution is uniform on $[0, q]$. $S'_{(r,2)}(c)$ is again given by expression Eq. (27), so a bidder with cost c_r inspects if $c_r \leq \hat{c}_{(r,2)} = q\left(1 - e^{-\lambda qr}\right)$. The (conditional) bid rate at $g = 1$ is $p_{(r,1)} = \lambda q$ while for $g = 2$ is

$$p_{(r,2)} = \lambda F(\hat{c}_{(r,2)})q = \lambda \left[z + (1 - z)\left(1 - e^{-\lambda qr}\right)\right] q \tag{46}$$

Using Eq. (70) we obtain the probability of no-bids at r.

$$P_{(r,2)} = e^{-\lambda q \int_{x=r}^{\tau} F(\hat{c}_{(x,2)})dx} \tag{47}$$

where

$$\int_{x=r}^{\tau} F(\hat{c}_{(x,2)})dx = \lambda q(\tau - r) - (1 - z)\left(e^{-\lambda qr} - e^{-\lambda q\tau}\right) \tag{48}$$

To compute S we need at least two bids from the start.

$$S = \int_{s=0}^{\tau} \left(e^{-\lambda q \int_{x=s}^{\tau} F(\hat{c}_{(x,2)})dx}\right) \lambda q F(\hat{c}_{(s,2)}) \left(1 - e^{-\lambda qs}\right) ds \tag{49}$$

Applying equation Eqs. (78) to (80) we can show that the profiles are decreasing.

If instead of uniform we use a linear density (quadratic c.d.f) with atom

$$F(c) = z + \frac{(1 - z)}{q^2} c^2 \tag{50}$$

we can show that the aggregate profile is strictly increasing for a large enough atom. A quick calculation from Eq. (78) shows us that

$$\begin{aligned} \dot{A}_r &= (\lambda q)^2 P_{(r,2)}(1 - z)\left(1 - S_{(r,1)}^2\right)\left[S_{(r,1)}\left(2 - S_{(r,1)}\right) - z\left(1 - S_{(r,1)}^2\right)\right] \\ &\propto S_{(r,1)}\left(2 - S_{(r,1)}\right) - z\left(1 + S_{(r,1)}\right)\left(1 - S_{(r,1)}\right) \end{aligned}$$

That is, the slope of bid intensity is proportional to the expression in brackets. Thus, the slope is negative (A_r time increasing) at rem r if

$$z \geq \underline{z}(r) \triangleq \frac{1 - e^{-2\lambda qr}}{e^{-\lambda qr}\left(2 - e^{-\lambda qr}\right)} \tag{51}$$

This cutoff is positive and increasing in the rem. Condition (51) is satisfied for all rems if it holds at the start, for a rem of τ. Therefore the profile is increasing for $r \geq \underline{z}(\tau)$. Note also that the atom is essential to get increasing since when $z = 0$ the condition does not hold for any $\tau > 0$. This last observation suggests us that the family of distribution that can give increasing profile is bimodal and carries some degree of convexity in the c.d.f.

Lemma 7. *(Attempted) For a uniform p.d.f with atom and full support, all profiles are decreasing, whereas for a linear p.d.f with atom and full support, there exists a low cutoff on the atom $\underline{z}(\tau)$, increasing in the campaign's length, that makes all profiles increasing.*

Proof of Lemma 7. (To be written) ■

4 Endogenous timing

In this section we relax the assumption that all bidders act only upon arrival and mostly present model and some profile predictions obtained under endogenous timing. For brevity, we refer to the new bidder type as endo while to that considered until now are exo. The key difference between them is that endos can postpone their choice of inspection and bidding to future periods. In particular, we make the assumption that they can only opt for delay their contingent choice of inspection and bidding to the last instant of activity, at rem $r = 0+\epsilon \equiv 0$. This follows from the idea that a continuous or periodic monitoring of the campaign is too costly, hence reduced to a single act. We also assume that bidders' inspection costs are drawn from the binary distribution $c_L = 0$, $c_H > 0$ with mass z on c_L presented in Section 3.4.

There are two key novelty with respect to what we saw so far. Firstly, we the possibility of waiting possibly combined with the necessity of inspecting before bidding makes bidders' waiting times strategic substitutes. This is a new strategic effect that combines with the fundamental strategic complementary between previous bidding and future inspections. Given that bidders do not observed who is waiting, they have to infer it from the history of nodes observed so far. To formulate their strategy, we consider nodes (r, g, l), where l is the highest number of bidders waiting in equilibrium. Under assumption Assumption 1, at each bidder r chooses among actions A,C,D, where action D means waiting and repeating the choice of A or C conditional on the observed gap g_0. The payoff from A is $u^A = 0$ and u^C is the same as Eq. (2). The payoff from choosing D is instead

$$u^D = \mathbb{1}_{g_{0+\epsilon} \geq \hat{g}_{(0)}} \left[u^C\right] = \mathbb{1}_{g_{0+\epsilon} \geq \hat{g}_{(0)}} \left\{\mathbb{1}_{g_0 \geq 0} \left(v_r - (v-d)\right)^+ - c_r\right\} \tag{52}$$

In this way, inspecting is conditional on observing a lower enough gap at the proximity of the end. This can give more safety on the success prospects but reduces inspection. The expected utility a bidder enjoys by waiting is the maximum of the value that he can obtain in the last round. Formally, with a unitary arrival at most, the (expected)utility bidder r enjoys is

$$U^D_{(r,g,l)} = \mathbb{E}_{(r,g,l+1,w_i=1)} V_{(r-1,g,l+1)} \tag{53}$$

where $V_{(r-1,g,l+1)} = \max_{a \in \{A,C\}} U_{(0,g_0,l_0;a_0=a)}$ is the highest value obtained from the last period inspection and obviously 0 in case of abstention. We look at cutoff strategy described by two cutoffs $c_H r, g, l^C \leq c_H r, g, l^D$ such that bidders choose C for $c \leq \hat{c}_{(r,g,l)}$; D for $c_H r, g, l^C < c \leq c_H r, g, l^D$ and A if $c > c_H r, g, l^D$, which coincides with the case of a frozen campaign.

Notice that in principle bidders can opt for a strategy of inspection and delayed bidding, however any strategy that considers such choice is dominated by others prescribing immediate bidding. To see this, note that after bidder r knows $v_r = \nu$ his objective is to choose when to bid to maximize the success rate. Given that early bidding and late inspecting are strategic complements, the best he can do is to to bid immediately after inspecting, inducing others to inspect and hence the success rate.

A second key novelty is the addition of larger initial bunching of m potential arrivals at rem $r = T$. These represents pre-aware bidders, such as contacts or friends, that have been informed by the entrepreneur (E) during the campaign's pitch, before it started. The purpose of introducing them is to be able to generate the dynamics underlying the widely commented U-shape pattern observed in practice. To do so, we look for a profile that is kick-started by contacts, drops, and then increases gradually until it peaks again at the end.

The presence of firends and contacts increases also the spectrum of potential nodes the campaign can reach. Within the campaign, each gap can be observed for a given number of potential funders waiting. Furthermore there can be multiple bids at the start.

letting $p_{(b;r,g,l)}$ is the probability of collecting b bids at node (r, g, l), we have

$$A_T = \sum_{b=0}^{m} p_{(b;T,K,0)} b \tag{54}$$

$$A_T^{\mathcal{S}} = \frac{1}{S} \left[\sum_{b=0}^{m} p_{(b;T,K,0)} S_{(T-1,K-b,l_{(b)})} b \right] \tag{55}$$

$$A_T^{\mathcal{F}} = \frac{1}{1-S} \left[\sum_{b=0}^{m} p_{(b;T,K,0)} (1 - S_{(T-1,K-b,l_{(b)})}) b \right] \tag{56}$$

with

$$S_{(T,K,l)} = \sum_{b=0}^{m} p_{(b;T,K,0)} S_{(T-1,K-b,l_{(b)})} \tag{57}$$

At a lower rem but before the very end, bidders are uncertain on how many are waiting. This puts different weights on the expected bid rates as follows:

$$A_r = \sum_{g=K-(T-r)}^{K} \sum_{l=0}^{T-r-K+g} P_{(r,g,l)} p_{(r,g,l)} \tag{58}$$

$$A_r^{\mathcal{S}} = \frac{1}{S} \sum_{g=K-(T-r)}^{K} \sum_{l=0}^{T-r-K+g} P_{(r,g,l)} \left[p_{(r,g,l)} S_{(r-1,g-1,l)} \right] \tag{59}$$

$$A_r^{\mathcal{F}} = \frac{1}{1-S} \sum_{g=K-(T-r)}^{K} \sum_{l=0}^{T-r-K+g} P_{(r,g,l)} \left[p_{(r,g,l)} (1 - S_{(r-1,g-1,l)}) \right] \tag{60}$$

We impose Pareto optimality at every subgame to rule out the coordination failure that can otherwise emerge.

4.1 Homogeneous inspection costs

Assume now that all bidders have the same inspection cost $c_r = c$ and arrive at a time rate of λ. Bidders form a belief on how many of their predecessors are waiting. To do so, we let l denote the number of times no bid is observed at some previous node where the equilibrium strategy prescribes waiting. For each of these occurrences, by Bayes' rule, future bidders attribute a probability λ to the event that a bidder arrived and waited. Therefore, from the point of view

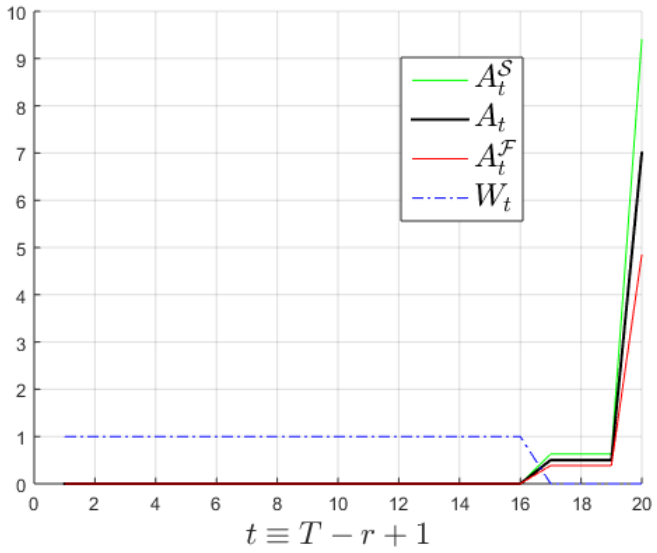

Figure 10: Bid and wait rates ($T = 20$, $K = 10$, $q = .5$, $c = .2$)

of an arriving bidder, the number of waiting bidders is binomially distributed with probability λ over a sample of size l. Moreover, since the outcome of each inspection is independent of the number of waiting bidders, it is as such also the number of bids collected. As a result of all waiting bidders deciding to play C simultaneously, the number of pledges collected in the last instant is binomially distributed over a sample of size at most l with probability λq. In this case the node-transition probabilities are determined as follows: at nodes where bidders play C we have

$$\begin{aligned} Q_{(r,g,l;r-1,g-1,l)} &= p_{(r,g,l)} \\ Q_{(r,g,l;r-1,g,l)} &= 1 - p_{(r,g,l)} \\ Q_{(r,g,l;r-1,g,l+1)} &= 0 \end{aligned}$$

when bidders rather play D we have instead $Q_{(r,g,l;r-1,g,l+1)} = 1$ and, when A is played, $Q_{(r,g,l;r-1,g,l)} = 1$.

Using this model we can easily predict an increasing profile when c is high, obtaining the opposite result from the same setting but under exogenous timing presented in Section 3.3. This is driven by free-riding by the early bidders who can go late if not very pivotal. The extent of free riding increases in c and with a higher K while reduces when duration increases. Fig. 10 shows a typical increasing profile with initial free-riding.

4.2 Binary inspection costs with $c_L = 0$ and $c_H > 0$

When we have instead $c_L = 0$ and $c_H > 0$, L-type will always play C upon arrival, as usual. Now l represents the highest number of H-type who choose to wait at nodes where $a_{(r,g,l;H)=D}$. Whenever bidders evaluate checking observing the history and observe no bid at a node where H-type might have waited, they form a belief on the probability that someone more is waiting, given by the probability that an H-type arrived relative to the event that nobody arrived or an

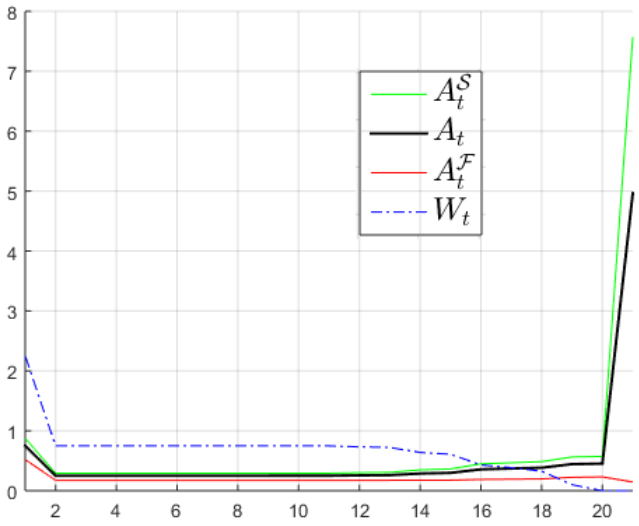

Figure 11: Bid and wait rates ($T = 20 + 1$, $K = 10$, $m = 3$, $q = .5$, $z = .5$ $c_H = .3$)

L-type who disliked the good arrived but abstained.

$$\mu(\lambda, z, q) = \frac{\lambda(1-z)}{(1-\lambda) + \lambda(z(1-q) + (1-z))} = \frac{\lambda(1-z)}{1-\lambda z q} \tag{61}$$

Notice that $\mu(\lambda, z, q)$ is decreasing in z and increasing in q: higher probability of L-type arriving as well as a lower probability that the first bidder likes the good leads to a higher probability weight to the event that an L-type arrived in the first period but did not pledge. Also, μ is increasing in λ it raises the probability of an arrival hence someone waiting.

With the addition of some initial bunching, the model can predict U-shape dynamics under cold start, when initially L-types but H-types wait. This pattern is characterized by a time decreasing waiting rate, which combined with an heating effect generates a gradual warm-up, as shown in Fig. 11.

This is not the only situation where bidding patterns can resemble a U-shape. In this case bidders wait initially, but we can also have bidders waiting in the middle due to the reduced optimism after observing bad news on the campaign's progress.

Remark 1. *Bidders incentive to play D rather than C is in general non-monotone in the rem. The reason is that, when the rem is low, time is running out so bidders do not gain from waiting. As more time available the incentive to free ride by playing D is reduced by the chance of making future bidders more optimistic and hence increasing the success rate by playing C.*

5 Conclusion

We have presented a highly parsimonious model of crowdfunding that is able to account for a variety of observed momentum effects in the dynamics of funding, including the much-commented U-shape profile. Of course, the reality is substantially more complex than our baseline model, which focuses on pure private values and bidders exogenously constrained to either bid in the

same period that they become aware of the project or fully abstain from bidding. However, as with our endogenous bidder extension, it is clear that the insights from our basic set-up readily extend to cover richer scenarios and to generate additional effects. Moreover, the basic model's simplicity is a virtue, since it allowed us to understand the driving dynamic forces despite the complexity of the challenge faced by bidders. They must anticipate how project success chances depend on the inspection calculus of all bidders who have not yet moved. Leaving aside the "friends" who enjoy looking at the entrepreneur's project, each bidder is only willing to dedicate any time or effort to inspecting a project if learning his type is useful. That, in turn, requires the project to have a chance of success. As a result, the distribution of inspection costs and bidder knowledge about those costs take centre-stage.

Crowdfunding campaigns have three key features: the threshold, the price (more generally, minimum price) and the duration. The difference between this threshold and the current funding aggregate, when divided by the price, determines the funding gap that later bidders must bridge before the deadline is reached (duration completed) in order for the project to succeed and for any benefits to accrue. However, it is not just the initial gap that matters, because bidders arrive over time and if the gap is too high relative remaining time, bidders may stop inspecting and the project may fizzle out. With a distribution of inspection costs, some bidders are relevant while others are not, in that their inspection-costs are prohibitive and they do not even consider bidding. Overall, projects are more likely to succeed the lower is the initial funding gap (threshold divided by price) relative to project duration and the inspection-cost adjusted bidder arrival rate.

Our study is incomplete but we can summarize some preliminary results.

For relatively high initial gaps, projects start in a cold state in that only lowest cost bidders are willing to inspect. If there is a sufficient mass of bidders with no cost of inspection, such projects are likely to end up in a hot state, and this draws in a greater rate of inspection and hence bids among later arrivals. The bidding rate profile is, therefore, increasing over time. Conversely, when the gap is initially relatively low, the project starts in a hot-state, but projects face a risk of falling out of their hot state. Such projects tend to exhibit a decreasing funding profile. Conditioning on project success and failure moderates these effects but they remain relevant.

Including the set of endogenously timed arrivals of friends and close contacts then allows us to explain the U-shaped profile in cases where projects start in a cold state. Loosely, given that project success rates on Kickstarter are generally under 50%, it is likely that a majority indeed begin in a cold state. So our model is broadly consistent with the U-shaped dynamics that initially motivated our study. In later drafts of this paper, we will conduct empirical tests to probe our understanding further.

The distribution of inspection costs also plays a major role. If there is an atom of this distribution at zero (or equivalently, if inspection costs can be negative in that bidders enjoy inspecting), then projects can more easily get hot after a cold start. If there is no such atom, the possibility for projects to grow over time is too small and the U-shape is not expected.

As we noted in the introduction, it will be important to allow for common value effects and advertising to account for the full wealth of possible dynamics. Common values readily generate positive and negative cascades but combining with the threshold effect in our dynamic

framework is far from trivial.

Advertising and project promotion effects are highly compatible with our model. Depending on the technology of advertising, it is likely that a lot could be gained from strategically-timed promotions that raise bidder arrival rates precisely when projects are at risk of going cold and dying out. Such an analysis would have to pay attention to bidders' awareness of the promotion strategies in use.

Our analysis is also relevant for entrepreneurs who need to evaluate how their strategic choices affect project success prospects. They know that raising price lowers the chance of a success. Our analysis shows that the resulting trade-off is significantly more complicated than simply assessing the initial gap ($\lceil T/p \rceil$), as sufficed in the static context with a single price. Dividing the gap by time available ($T/p\tau$) is a natural first look in a setting where bidders arrive over the duration of the project, but inspection costs can relegate many potential bidders into mere irrelevancies who pass over the project if the gap when they come across the project is too high relative to the remaining time available on the campaign clock.

References

Agrawal, A., Catalini, C., and Goldfarb, A. (2014). Some simple economics of crowdfunding. *Innovation Policy and the Economy*, 14(1):63–97.

Agrawal, A. K., Catalini, C., and Goldfarb, A. (2011). The geography of crowdfunding. Technical report, National bureau of economic research.

Alaei, S., Malekian, A., and Mostagir, M. (2016). A dynamic model of crowdfunding.

Babich, V., Tsoukalas, G., and Marinesi, S. (2017). Does crowdfunding benefit entrepreneurs and venture capital investors?

Belleflamme, P., Lambert, T., and Schwienbacher, A. (2014). Crowdfunding: Tapping the right crowd. *Journal of business venturing*, 29(5):585–609.

Cason, T. N. and Zubrickas, R. (2018). Crowdfunding for public goods with refund bonuses: An empirical and theoretical investigation.

Chakraborty, S. and Swinney, R. (2018). Designing rewards-based crowdfunding campaigns for strategic contributors. *Available at SSRN 3240094*.

Chang, J.-W. (2016). The economics of crowdfunding.

Chemla, G. and Tinn, K. (2018). Learning through crowdfunding. *Available at SSRN 2796435*.

Colombo, M. G., Franzoni, C., and Rossi-Lamastra, C. (2015). Internal social capital and the attraction of early contributions in crowdfunding. *Entrepreneurship theory and practice*, 39(1):75–100.

Cordova, A., Dolci, J., and Gianfrate, G. (2015). The determinants of crowdfunding success: evidence from technology projects. *Procedia-Social and Behavioral Sciences*, 181:115–124.

Crosetto, P. and Regner, T. (2018). It's never too late: funding dynamics and self pledges in reward-based crowdfunding. *Research Policy*, 47(8):1463–1477.

Deb, J., Öry, A., and Williams, K. (2018). Aiming for the goal : Contribution dynamics of crowdfunding.

Du, L., Hu, M., and Wu, J. (2017). Contingent stimulus in crowdfunding.

Ellman, M. and Hurkens, S. (2019a). Fraud tolerance in optimal crowdfunding. *Economics Letters*, 181(C):11–16.

Ellman, M. and Hurkens, S. (2019b). Optimal crowdfunding design. *forthcoming Journal of Economic Theory*.

Hu, M., Li, X., and Shi, M. (2015). Product and pricing decisions in crowdfunding. *Marketing Science*, 34(3):331–345.

Kuppuswamy, V. and Bayus, B. L. (2017). Crowdfunding creative ideas: The dynamics of project backers in kickstarter. *A shorter version of this paper is in" The Economics of Crowdfunding: Startups, Portals, and Investor Behavior"-L. Hornuf and D. Cumming (eds.)*.

Kuppuswamy, V. and Bayus, B. L. (2018). 17. a review of crowdfunding research and findings. *Handbook of Research on New Product Development, Golder, PN, and Mitra, D.(Eds.), Cheltenham, UK: Edward Elgar Publishing*, pages 361–373.

Liu, S. (2018). A theory of collective investment with application to venture funding.

Ma, C.-T. A. and Manove, M. (1993). Bargaining with Deadlines and Imperfect Player Control. *Econometrica*, 61(6):1313–1339.

Mollick, E. (2014). The dynamics of crowdfunding: An exploratory study. *Journal of business venturing*, 29(1):1–16.

Moritz, A. and Block, J. H. (2016). Crowdfunding: A literature review and research directions. In *Crowdfunding in Europe*, pages 25–53. Springer.

Rao, H., Xu, A., Yang, X., and Fu, W.-T. (2014). Emerging dynamics in crowdfunding campaigns. In *International Conference on Social Computing, Behavioral-Cultural Modeling, and Prediction*, pages 333–340. Springer.

Shen, W., Crandall, J. W., Yan, K., and Lopes, C. V. (2018). Information design in crowdfunding under thresholding policies. In *Proceedings of the 17th International Conference on Autonomous Agents and MultiAgent Systems*, pages 632–640. International Foundation for Autonomous Agents and Multiagent Systems.

Short, J. C., Ketchen Jr, D. J., McKenny, A. F., Allison, T. H., and Ireland, R. D. (2017). Research on crowdfunding: Reviewing the (very recent) past and celebrating the present. *Entrepreneurship Theory and Practice*, 41(2):149–160.

Solomon, J., Ma, W., and Wash, R. (2015). Don't wait!: How timing affects coordination of crowdfunding donations. In *Proceedings of the 18th acm conference on computer supported cooperative work & social computing*, pages 547–556. ACM.

Strausz, R. (2017). A theory of crowdfunding: A mechanism design approach with demand uncertainty and moral hazard. *American Economic Review*, 107(6):1430–76.

Vismara, S. (2016). Information cascades among investors in equity crowdfunding. *Entrepreneurship Theory and Practice*.

Zhang, J. (1997). Strategic delay and the onset of investment cascades. *The RAND Journal of Economics*, pages 188–205.

Zhang, J. and Liu, P. (2012). Rational herding in microloan markets. *Management science*, 58(5):892–912.

Zhang, J., Savin, S., and Veeraraghavan, S. (2017). Revenue management in crowdfunding.

Appendices

Appendix A Continuous time

This section presents the continuous limit of the model of Section 2, where every round becomes n sub-rounds of length $1/n$ with a bidder arrival probability $\lambda/n = 1/n$. To distinguish from the discrete setting, we denote the deadline by τ so time remaining $r \in [0, \tau]$. In continuous time, $p_{(r,g)} = qF(qc_H r, g)$ is the instantaneous rate of bidding, or *bid intensity*, at node (r, g), which can be seen as the probability of an instantaneous shift in gap and determines the transition probabilities as follows

$$Q_{(r,g;r+dr,g_{r+dr})} = \begin{cases} p_{(r,g)}dr + o(dr) & \text{for } g_{r+dr} = g \\ 1 - p_{(r,g)}dr + o(dr) & \text{for } g_{r+dr} = g-1 \\ o(dr) & \text{for } g_{r+dr} =\leq g-2 \end{cases} \tag{62}$$

and satisfies the condition that $Q_{(r,g;r,g)} = 1$ and $Q_{(r,g;s,g')} = 0$ for $s > r$ or $g < g'$. This operator can be use to construct time densities of different bid events. For example, the density of no bids between two future rems can be computed as

$$Q_{(r,g;s-dr,g)} = Q_{(r,g;s,g)}Q_{(s,g;s-dr,g)} = Q_{(r,g;s,g)}\left(1 - p_{(s,g)}dr\right) + o(dr) \tag{63}$$

$$\implies D_s\left[Q_{(r,g;s,g)}\right] = \lim_{dr\to 0} \frac{Q_{(r,g;s,g)} - Q_{(r,g;s-dr,g)}}{dr} = -Q_{(r,g;s,g)}p_{(s,g)} \tag{64}$$

where D is the derivative with respect to the future rem s. The solution of this o.d.e is given by

$$Q_{(r,g;s,g)} = e^{-\int_{x=s}^{r} p_{(x,g)}dx} + const. \tag{65}$$

where from the end-point condition $Q_{(r,g;r,g)} = 1 = e^0 + const$, so $const = 0$.

In an infinitesimal interval $(r - dr, r]$, the campaign's funding gap falls by one unit with probability $p_{r,g}dr$ and otherwise stays the same; other transitions have probability of order dr^2 and can be neglected. Using dots to denote partial differentiation with respect to r, this implies,

$$S_{(r+dr,g)} = p_{(r,g)}drS_{(r,g-1)} + (1 - p_{(r,g)}dr)S_{(r,g)} + o(dr) \tag{66}$$

$$\implies \dot{S}_{(r,g)} = \lim_{dr\to 0} \frac{S_{(r+dr,g)} - S_{(r,g)}}{dr} = p_{(r,g)} \left(S_{(r,g-1)} - S_{(r,g)}\right) \tag{67}$$

Intuitively, increasing r raises the success rate because having marginally more time raises the chance that a bidder arrives, inspects and bids, which lowers g by one unit which raises the success rate by $S_{(r,g-1)} - S_{(r,g)}$. This differential equation is the continuous-time analogue of the martingale property that governs $S_{(r,g)}$. Similarly, the probability P of reaching state (r, g) obeys the differential equation,[19]

$$P_{(r-dr,g)} = P_{(r,g)} \left(1 - p_{(r,g)}dr\right) + P_{(r,g+1)}p_{(r,g+1)}dr + o(dr) \tag{68}$$

$$\implies \dot{P}_{(r,g)} = \lim_{dr\to 0} \frac{P_{(r,g)} - P_{(r-dr,g)}}{dr} = P_{(r,g)}p_{(r,g)} - P_{(r,g+1)}p_{(r,g+1)} \tag{69}$$

In sum, the differential equations,

$$\begin{aligned} \dot{P}_{(r,g)} &= P_{(r,g)}p_{(r,g)} - P_{(r,g+1)}p_{(r,g+1)} \\ \dot{S}_{(r,g)} &= p_{(r,g)} \left(S_{(r,g-1)} - S_{(r,g)}\right) \end{aligned} \tag{70}$$

determine the values of $S_{(r,g)}$ and $P_{(r,g)}$ in all states once combined with the endpoint conditions,

$$\begin{aligned} S_{(0,g)} &= 0 \text{ if } g_0 > 0 \\ S_{(0,g)} &= 1 \text{ if } g_0 \leq 0 \end{aligned} \qquad\qquad P_{(\tau,K)} = 1 \tag{71}$$

For the $K = 2$ example we solve throughout the paper, bidding intensities at rem r can be expressed as

$$A_r = \lambda q \left[1 - P_{(r,2)} \left(1 - F(\hat{c}_{(r,2)})\right)\right] \tag{72}$$

$$A_r^{\mathcal{S}} = \frac{1}{S}\lambda q \left[1 - P_{(r,2)} \left(1 - F(\hat{c}_{(r,2)})S_{(r,1)}\right)\right] \tag{73}$$

$$A_r^{\mathcal{F}} = \frac{1}{1-S}\lambda q \left[P_{(r,2)}F(\hat{c}_{(r,2)}) \left(1 - S_{(r,1)}\right)\right] \tag{74}$$

[19] The campaign almost always reaches state (r, g) by passing through a state "just" prior to it with the same gap and no intervening bid, or a gap one unit higher and a single intervening bid.

The slopes with respect to the rem are derived using the product rule

$$\dot{A}_r = \lambda q \left[-\dot{P}_{(r,2)} + \dot{P}_{(r,2)} F(\hat{c}_{(r,2)}) + P_{(r,2)} \dot{F}\left(\hat{c}_{(r,2)}\right) \right] \tag{75}$$

$$\dot{A}_r^{\mathcal{S}} = \frac{1}{S} \lambda q \left[-\dot{P}_{(r,2)} + \dot{P}_{(r,2)} F(\hat{c}_{(r,2)}) S_{(r,1)} + P_{(r,2)} \dot{F}\left(\hat{c}_{(r,2)}\right) S_{(r,1)} + P_{(r,2)} F(\hat{c}_{(r,2)}) \dot{S}_{(r,1)} \right] \tag{76}$$

$$\dot{A}_r^{\mathcal{F}} = \frac{1}{1-S} \lambda q \left[\dot{P}_{(r,2)} F\left(\hat{c}_{(r,2)}\right) \left(1 - S_{(r,1)}\right) + P_{(r,2)} \dot{F}\left(\hat{c}_{(r,2)}\right) \left(1 - S_{(r,1)}\right) - P_{(r,2)} F(\hat{c}_{(r,2)}) \dot{S}_{(r,1)} \right] \tag{77}$$

We can simplify further using Eq. (70) and Eq. (69) we have $\dot{P}_{(r,2)} = P_{(r,2)} p_{(r,2)}$ and $\dot{S}_{(r,1)} = p_{(r,1)} \left(1 - S_{(r,1)}\right)$.

$$\dot{A}_r = \lambda q P_{(r,2)} \left[\dot{F}\left(\hat{c}_{(r,2)}\right) - p_{(r,2)} \left(1 - F(\hat{c}_{(r,2)})\right) \right] \tag{78}$$

$$\dot{A}_r^{\mathcal{S}} = \frac{1}{S} \lambda q P_{(r,2)} \left[p_{(r,1)} \left(1 - S_{(r,1)}\right) F\left(\hat{c}_{(r,2)}\right) - p_{(r,2)} \left(1 - F(\hat{c}_{(r,2)}) S_{(r,1)}\right) + \dot{F}\left(\hat{c}_{(r,2)}\right) S_{(r,2)} \right] \tag{79}$$

$$\dot{A}_r^{\mathcal{F}} = \frac{1}{1-S} \lambda q P_{(r,2)} \left(1 - S_{(r,1)}\right) \left[\dot{F}\left(\hat{c}_{(r,2)}\right) + F\left(\hat{c}_{(r,2)}\right) \left(p_{(r,2)} - p_{(r,1)}\right) \right] \tag{80}$$

Appendix B Additional derivations

Conditional bid intensities under hot start with $K = 2$:

$$A_r^{\mathcal{S}} = \begin{cases} \frac{1}{S} \lambda q \underbrace{\left(1 - e^{-\lambda q \tau}\right)}_{S_{(r,1)}} & \text{for } r \geq \hat{r}_{(2)} \\ \frac{1}{S} \lambda q \left[1 - \underbrace{e^{-\lambda q (\tau - \hat{r}_{(2)}(1-z) - zr)}}_{1-\pi_r} \left(1 - z \underbrace{\left(1 - e^{-\lambda q r}\right)}_{S_{(r,1)}} \right) \right] & \text{for } r < \hat{r}_{(2)} \end{cases} \tag{81}$$

$$A_r^{\mathcal{F}} = \begin{cases} \frac{1}{1-S} \left[\lambda q \underbrace{\left(e^{-\lambda q r}\right)}_{1-S_{(r,1)}} \right] & \text{for } r \geq \hat{r}_{(2)} \\ \frac{1}{1-S} \left[\underbrace{e^{-\lambda q (\tau - \hat{r}_{(2)}(1-z) - zr)}}_{1-\pi_r} \lambda z q \underbrace{\left(e^{-\lambda q r}\right)}_{1-S_{(r,1)}} \right] & \text{for } r < \hat{r}_{(2)} \end{cases} \tag{82}$$

Appendix C Proofs of main propositions

Proof of Proposition 1. We prove this by backward induction, starting from the final action period $r = 1$. $U_{r=1,g}^{C} = q S_{0,g-1} - c_i$ which equals $q - c_i$ if $g \leq 1$ and $-c_i$ if $g > 1$. So $\hat{c}_{1,g\leq 1} = q$ and $\hat{c}_{1,g>1} = 0$. Also, $S_{1,g} = 0$, for $g > 1$, $S_{1,1} = F(q)$, $S_{1,g} = 1$ for $g < 1$.

Suppose that for all later rounds $r-1, r-2, ..., 1$, bidders play C if $c_i \leq \hat{c}_{r-1,g_{r-1}}$ for all possible $g_{r-1}, ..., g_1$. Then in round r, we have $U_{r,g}^{C} = q S_{r-1,g-1} - c_i$. By the inductive hypothesis, we have $S_{r-1,g-1} = qF(\hat{c}_{r-1,g-1}) S_{r-2,g-2} + (1 - qF(\hat{c}_{r-1,g-1})) S_{r-2,g-1}$, which is constant w.r.t.

c_i. Thus, since i's utility function is linear in c_i, he finds optimal to play C if and only if $c_i \leq \hat{c}_{r,g} = qS_{r-1,g-1}$. ■

Proof of Lemma 1. For proving part (i), define the mapping $S_r(g) : g \mapsto S_{r,g}$ for $g \in \{K-T, K\}$. The claim holds if $S_r(.)$ is non-increasing for all r. We proceed by induction on r. Base case: $r = 0$. Using expression 11, it is obvious that $S_0(.)$ is decreasing. Induction: Assume $S_{r-1}(.)$ is decreasing. Using expression 11 and expanding $p_{r,g}$ we obtain

$$S_r(g) = S_{r-1}(g) + qF\left(qS_{r-1}(g-1)\right) \cdot \left[S_{r-1}(g-1) - S_{r-1}(g)\right] \tag{83}$$

Subtracting $S_r(g-1)$ from $S_r(g)$ and rearranging the expression we obtain

$$\begin{aligned} S_r(g) - S_r(g-1) &= \left[S_{r-1}(g) - S_{r-1}(g-1)\right] \cdot \left(1 - qF(qS_{r-1}(g-1))\right) \\ &+ \left[S_{r-1}(g-1) - S_{r-1}(g-2)\right] \cdot qF(qS_{r-1}(g-2)) \end{aligned} \tag{84}$$

which is non-positive for all g by the inductive hypothesis.

For proving part (ii), define the mapping $S_g(r) : r \mapsto S_{r,g}$ for $r \in \{0, \ldots, T\}$. Our claim holds if $S_g(.)$ is non-decreasing for all g. We proceed by construction. If $g \leq 0$ we have $S_{g\leq 0}(r) = 1$ for all r, which is constant. For other values of g, manipulate expression 83 to obtain

$$S_g(r) - S_g(r-1) = qF(qS_{g-1}(r-1)) \cdot \left[S_{g-1}(r-1) - S_g(r-1)\right] \tag{85}$$

From part (i) of the lemma, we know that $S_{g-1}(r-1) - S_g(r-1)$ is non-negative, hence the whole expression is non-negative for any given g. We can conclude that $S_g(.)$ is non-decreasing.

For part (iii), note that $S_{r,g} = p_{r,g}S_{r-1,g-1} + (1-p_{r,g})S_{r-1,g} < S_{r-1,g}$ by part (ii) ■

Proof of Lemma 2. At a given state (r, g), the heat is $p_{(r,g)}$. In the following round, $g_{r-1} = g$ with probability $1 - p_{(r,g)}$ and $g_{r-1} = g - 1$ with probability $p_{(r,g)}$. In these adjacent states the (conditional) bid rate is $p_{(r-1,g-1)}$ and $p_{(r-1,g)}$. Applying the law of total probability, we find that

$$\mathbb{E}_{(r,g)}[p_{(r-1,g_{r-1})}] = p_{(r,g)}p_{(r-1,g-1)} + (1 - p_{(r,g)})p_{(r-1,g-1)} \tag{86}$$

Taking expectations over possible realisations of g according to Equation (58), we obtain the difference in (unconditional) bid rates

$$\begin{aligned} A_{r-1} - A_r &= \sum_{g=K-(T-r)}^{K} P_{(r,g)} \left[(1 - p_{(r,g)})p_{(r-1,g)} - p_{(r,g)}(1 - p_{(r-1,g-1)})\right] \\ &= \mathbb{E}_g \left[\Delta_{(r,g)}\right] \end{aligned} \tag{87}$$

We analyse now successful projects. Using Equation (11), we expand $S_{(r-1,g-1)}$ to obtain

$$S_{(r-1,g-1)} = p_{(r-1,g-1)}S_{(r-2,g-2)} + \left(1 - p_{(r-1,g-1)}\right) S_{(r-2,g-1)} \tag{88}$$

Substituting into Eq. (59) we get

$$A_r^{\mathcal{S}} = \frac{1}{S} \sum_{g=K-(T-r)}^{K} P_{(r,g)} \left[p_{(r,g)} \left(p_{(r-1,g-1)}S_{(r-2,g-2)} + (1 - p_{(r-1,g-1)})S_{(r-2,g-1)}\right)\right] \tag{89}$$

and evaluated at $r-1$ and using 12 is

$$A^{\mathcal{S}}_{r-1} = \frac{1}{S} \sum_{g=K-(T-r)}^{K} P_{(r,g)} \left[p_{(r,g)} p_{(r-1,g-1)} S_{(r-2,g-2)} + (1-p_{(r,g)}) p_{(r-1,g)} S_{(r-2,g-1)} \right] \tag{90}$$

taking differences

$$\begin{aligned} A^{\mathcal{S}}_{r-1} - A^{\mathcal{S}}_{r} &= \frac{1}{S} \sum_{g=K-(T-r)}^{K} P_{(r,g)} \left[\left((1-p_{(r,g)}) p_{(r-1,g)} - p_{(r,g)} (1-p_{(r-1,g-1)}) \right) S_{(r-2,g-1)} \right] \\ &= \mathbb{E}_g \left[\Delta_{(r,g)} \mid \mathcal{S} \right] \end{aligned} \tag{91}$$

Finally, for failed projects, we use expression 11 to obtain

$$1 - S_{(r-1,g-1)} = p_{(r-1,g-1)} \left(1 - S_{(r-2,g-2)} \right) + (1-p_{(r-1,g-1)}) \left(1 - S_{(r-2,g-1)} \right) \tag{92}$$

Computing the difference between expression Eq. (60) at $r-1$ and Eq. (60) at r after substituting Eq. (92)

$$\begin{aligned} A^{\mathcal{F}}_{r-1} - A^{\mathcal{F}}_{r} &= \frac{1}{1-S} \sum_{g=K-(T-r)}^{K} P_{(r,g)} \left[\left((1-p_{(r,g)}) p_{(r-1,g)} - p_{(r,g)} (1-p_{(r-1,g-1)}) \right) (1 - S_{(r-2,g-1)}) \right] \\ &= \mathbb{E}_g \left[\Delta_{(r,g)} \mid \mathcal{F} \right] \end{aligned} \tag{93}$$

■

Proof of Lemma 3. Part (i). Note that, by definition, $\hat{g}_{(r)}$ satisfies. By definition, $\hat{g}_{(r)}$ has to satisfy

$$S_{(r,\hat{g}_{(r)})} \geq \frac{c}{q} > S_{(r,\hat{g}_r+1)} \tag{94}$$

$$S_{(r-1,\hat{g}_{(r-1)})} \geq \frac{c}{q} > S_{(r-1,\hat{g}_{(r-1)}+1)} \tag{95}$$

Since $S_{r,g}$ is increasing in r and by Inequality (95) $S_{r-1,\hat{g}_{(r)}+1} < c/q$. Then, because $S_{(r,g)}$ is decreasing in g, the only way to satisfy simultaneously (94) and (95) is by having $\hat{g}_{(r-1)} \leq \hat{g}_r$.

Part (ii) is an immediate consequence of the martingale property. By Eq. (20), $S_{r-1,\hat{g}_{(r)}-1} \geq c/q$. If $\hat{g}_{(r-1)} < \hat{g}_r - 1$ then $S_{r-2,\hat{g}_{(r)}-2} < c/q$ but also $S_{r-1,\hat{g}_{(r)}-1} = S_{r-2,\hat{g}_r-1} + p_{r-1,\hat{g}_{(r)}-1}(S_{r-2,\hat{g}_{(r)}-2} - S_{r-2,\hat{g}_{(r)}-1}) < c/q$, a contradiction.

Part (iii) By induction on r. Base step: $r=2$. $\hat{g}_{(1)} \in \{1, -\infty\}$. $\hat{g}_{(1)} = -\infty$, clearly implies $\hat{g}_{(r)} = -\infty$ for all r hence

$$S_{(2,g|\hat{g}_{(1)}=1)} \geq S_{(2,g|\hat{g}_{(1)}=-\infty)} = \begin{cases} 1 & \text{if } g \leq 0 \\ 0 & \text{otw.} \end{cases}$$

Induction: Assume $S_{(r,g|\hat{\boldsymbol{g}}_{\boldsymbol{r-1}})} \geq S_{(r,g|\hat{\boldsymbol{g}}'_{\boldsymbol{(r-1)}})}$ for all (r,g). By definition,

$$S_{(r+1,g|\hat{\boldsymbol{g}}'_{\boldsymbol{(r)}})} = p_{(r+1,g)} S_{(r,g-1|\hat{\boldsymbol{g}}'_{\boldsymbol{(r-1)}})} + (1 - p_{(r+1,g)}) S_{(r,g|\hat{\boldsymbol{g}}'_{\boldsymbol{(r-1)}})}$$

Since $S_{(r,g-1|\hat{\boldsymbol{g}}_{\boldsymbol{(r-1)}})} \geq S_{(r,g-1|\hat{\boldsymbol{g}}'_{\boldsymbol{(r-1)}})}$ and $S_{(r,g|\hat{\boldsymbol{g}}_{\boldsymbol{(r-1)}})} \geq S_{(r,g|\hat{\boldsymbol{g}}'_{\boldsymbol{(r-1)}})}$ by the inductive hypothesis,

$$S_{(r+1,g|\hat{\boldsymbol{g}}_{\boldsymbol{(r)}})} = p_{(r+1,g)} S_{(r,g-1|\hat{\boldsymbol{g}}_{\boldsymbol{(r-1)}})} + (1 - p_{(r+1,g)}) S_{(r,g|\hat{\boldsymbol{g}}_{\boldsymbol{(r-1)}})} \geq S_{(r+1,g|\hat{\boldsymbol{g}}'_{\boldsymbol{(r)}})}$$

Part (iv). Proof by induction on r. Let $\hat{g}_{(r)}$ and $\hat{g}'_{(r)}$ denote the gap threshold in round r for $c_i = c, c'$. Base step: $r = 1$. $\hat{g}_{(1)} = 1$ if $c \leq q$, $\hat{g}_{(1)} = -\infty$ otherwise. Clearly $c' > c$ implies $\hat{g}'_{(1)} \leq \hat{g}_{(1)}$. Induction: assume $\hat{\boldsymbol{g}}'_{\boldsymbol{(r)}} \leq \hat{\boldsymbol{g}}_{\boldsymbol{r}}$. At $r+1$, $S_{(r,\tilde{g}_{(r+1)}-1|\hat{\boldsymbol{g}}_{\boldsymbol{(r)}})} = \frac{c}{q}$. By (iii), $S_{(r,\tilde{g}_{(r+1)}-1|\hat{\boldsymbol{g}}'_{\boldsymbol{(r)}})} \leq \frac{c}{q} < \frac{c'}{q}$, hence $\tilde{g}'_{(r+1)} < \tilde{g}_{(r+1)}$ and $\hat{g}'_{(r+1)} \leq \hat{g}_{(r+1)}$. ■

Proof of Lemma 4. For any given r, π_r and π_{r-1} are related to each recursively. To see this, note that expanding $P_{(r,g)}$ using the recursive relation (12) we can express π_{r-1} as[20]

$$\pi_{r-1} = \sum_{g=K-T+(r-1)}^{\hat{g}_{(r-1)}} P_{(r-1,g)} \tag{96}$$

$$= \sum_{g=K-T+(r-1)}^{\hat{g}_{(r-1)}} P_{(r,g)}(1 - p_{(r,g)}) + P_{(r,g+1)} p_{(r,g+1)} \tag{97}$$

$$= \left(\sum_{g=K-T+r}^{\hat{g}_{(r-1)}} P_{(r,g)} \right) + P_{(r,\hat{g}_{(r-1)}+1)} p_{(r,\hat{g}_{(r-1)}+1)} \tag{98}$$

From Lemma 3, we know that $\hat{g}_{(r-1)} \in \{\hat{g}_{(r)}, \hat{g}_{(r)} - 1\}$. If $\hat{g}_{(r-1)} = \hat{g}_r$, $p_{(r,\hat{g}_{(r-1)}+1)} = 0$, and we can see that $\pi_{r-1} = \pi_r$. On the other hand, if $\hat{g}_{(r-1)} = \hat{g}_r - 1$, $p_{(r,\hat{g}_{(r-1)}+1)} = q$ and so $\pi_r - \pi_{r-1} = P_{(r,\hat{g}_{(r-1)}+1)}(1-q)$. Summarizing,

$$\pi_{r-1} - \pi_r = \begin{cases} 0 & \text{if } \hat{g}_{(r-1)} = \hat{g}_{(r)} \\ -P_{(r,\hat{g}_{(r-1)}+1)}(1-q) & \text{if } \hat{g}_{(r-1)} = \hat{g}_{(r)} - 1 \end{cases} \tag{99}$$

Hence π_r is decreases over time. ■

Proof of Proposition 2.

At a given node, a the relevant paths to determine how heats vary pass from vertices Start (r,g), Late $(r-1,g)$, Early $(r-1,g-1)$ and End $(r-2,g-1)$, though End is not needed here. We can have either the first three with the same heat, in which case $\Delta_{(r,g)} = 0$, or heats can be $h_{(r,g)} = \{c\}$, $h_{(r-1,g)} = \{\varnothing\}$, $h_{(r-1,g-1)} = \{c\}$. This is the only cases where heats can change since $h_{(r,g)} = \{\varnothing\}$ at start makes the campaign frozen afterwards and $h_{(r,g)} = \{c\}$ implies $h_{(r-1,g-1)} = \{c\}$ as well. in this case, $\Delta_{(r,g)}$ is clearly strictly negative since the late path from Start-Late-End cannot arise as moving to Late implies freezing the project. Formally,

$$\Delta_{(r,g)} = (1-\lambda q)0 - (\lambda q)(1-\lambda q) = -\lambda q(1-\lambda q) < 0 \tag{100}$$

[20] There are no positive terms with round indexed $(r-1)$ in Eq. (97) because $P_{(r,K-T+(r-1))} = 0$.

■

Proof of Proposition 3. Part (i). At a given r, either $\hat{g}_{(r-1)} = \hat{g}_{(r)}$ or $\hat{g}_{(r-1)} = \hat{g}_{(r)} - 1$. In the first case $\Delta_{(r,\hat{g}_{(r)}+1)} = zq^2(1-z) > 0$ and $\Delta_{(r,g)} = 0$ for $g \neq \hat{g}_{(r)} + 1$. In the other case, $\Delta_{(r,\hat{g}_{(r)})} = -q(1-q)(1-z) < 0$ and $\Delta_{(r,\hat{g}_{(r)})} = 0$ for $g \neq \hat{g}_{(r)}$. Thus, at a given r, either $\Delta_{(r,g_r)} \leq 0$ for all g_r or $\Delta_{(r,g_r)} \geq 0$ for all g_r. The result follows immediately applying Corollary 1.

Part (ii). Consider $c \in \left(0, q^K\right]$. This ensures $\hat{g}_{(r)}(\hat{\boldsymbol{g}}_{\boldsymbol{(r-1)}}) = r$ for $r \leq K$ and clearly $\hat{g}_{(r)}(\hat{\boldsymbol{g}}_{\boldsymbol{(r-1)}}) = K$ for $T \geq r > K$. Thus $\Delta_{(r,g)} \leq 0$ for all (r,g) such that $P_{(r,g)} > 0$, hence the profile is decreasing.

Now take $c \in \left(q(1-(1-q)^{T-K}), q\right]$. Then $\hat{g}_{(r)} = 1$ for all $r \leq T-K+2$ because $\hat{c}_{(T-K+2,2)} = q(1-(1-q)^{T-K+1}) > c$. At $r = T-K+3$, $g_{T-K+3} \geq 3$. Note $c > \hat{c}_{(T-K+2,2)}(\hat{\boldsymbol{g}}_{\boldsymbol{T-K+1}})$ implies $c > \hat{c}_{(r,g)}(\hat{\boldsymbol{g}}_{\boldsymbol{r-1}})$ for $T \geq r \geq T-K+3$. Thus the campaign gets hot only at $g_r = 1$. As a consequence, $\Delta_{(r,g)} \geq 0$ for all (r,g) such that $P_{(r,g)} > 0$ and clearly the profile is increasing.

In any case outside the previous two, there exist two periods r and r' such that $\Delta_{(r,g_r)} \geq 0$ for all g_r and $\Delta_{(r',g_{r'})} \leq 0$ for all $g_{r'}$. ■

Proof of Proposition 4. We apply Corollary 1, we know that the profile is decreasing if the following inequality holds:

$$\frac{\min\{S_{(r-1,g-1)}, 1/fq\} - \min\{S_{(r-2,g-1)}, 1/fq\}}{\min\{S_{(r-2,g-2)}, 1/fq\} - \min\{S_{(r-2,g-1)}, 1/fq\}} \geq q[z + (1-z)fq \min\{S_{(r-1,g-1)}, 1/fq\}] \quad (101)$$

From lemma 1, $S_{(r-2,g-2)} \geq S_{(r-1,g-1)} \geq S_{(r-2,g-1)}$; thus, depending on fq, we distinguish four cases:

i $fq \leq 1/S_{(r-2,g-2)}$

ii $1/S_{(r-2,g-2)} \leq fq \leq 1/S_{(r-1,g-1)}$

iii $1/S_{(r-1,g-1)} \leq fq \leq 1/S_{(r-2,g-1)}$

iv $fq \geq 1/S_{(r-2,g-1)}$

Case (i): For $fq \leq 1$, Eq. (101) reduces to

$$\frac{S_{(r-1,g-1)} - S_{(r-2,g-1)}}{S_{(r-2,g-2)} - S_{(r-2,g-1)}} \geq q[z + (1-z)fqS_{(r-1,g-1)}] \quad (102)$$

which is equivalent to

$$S_{(r-1,g-1)} - S_{(r-2,g-1)} \geq q[z + (1-z)fqS_{(r-1,g-1)}](S_{(r-2,g-2)} - S_{(r-2,g-1)})$$

From the definition of $S_{r,g}$ evaluated at $(r-1, g-1)$ we obtain

$$S_{(r-1,g-1)} - S_{(r-2,g-1)} = q[z + (1-z)fqS_{(r-2,g-2)}](S_{(r-2,g-2)} - S_{(r-2,g-1)})$$

and since $S_{(r-2,g-2)} \geq S_{(r-1,g-1)}$ by lemma 1, we can conclude that the profile is decreasing in time. The more general case of $fq \leq 1$ is presented

Case (ii): $\min\{S_{(r-2,g-2)}, 1/fq\} = 1/fq$. Eq. (101) becomes

$$S_{(r-1,g-1)} - S_{(r-2,g-1)} \geq q[z + (1-z)fqS_{(r-1,g-1)}] \left(\frac{1}{fq} - S_{(r-2,g-1)}\right)$$

and Eq. (11) evaluated at $(r-1, g-1)$ is given by

$$S_{(r-1,g-1)} - S_{(r-2,g-1)} = q\left(S_{(r-2,g-2)} - S_{(r-2,g-1)}\right)$$

and since $S_{(r-2,g-2)} \geq 1/fq$ by assumption, we conclude that the profile is decreasing.

Case (iii): $\min\{S_{(r-2,g-2)}, 1/fq\} = \min\{S_{(r-2,g-2)}, 1/fq\} = 1/fq$. Eq. (101) reduces to $1 \geq q$ which holds since $q \in (0,1)$.

Case (iv): Bidders are always willing to inspect; thus $p_{r,g} = q$ for all r, g. As a result, condition 1 holds with equality and bidding profiles are flat.

We conclude that the bidding profile resulting from a uniform $[0, 1/f]$ distribution of costs are weakly decreasing in time. ■

Appendix D Additional figures

Figure 12: Graphical representation of Corollary 1

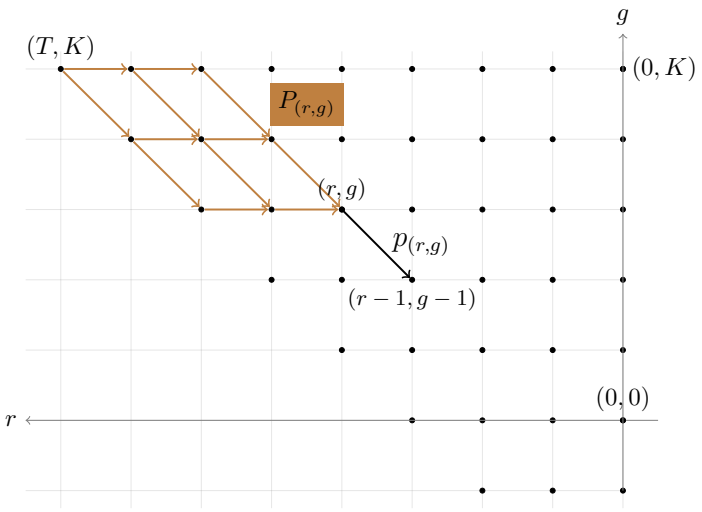

(i) Cooling and heating effect along adjacent nodes

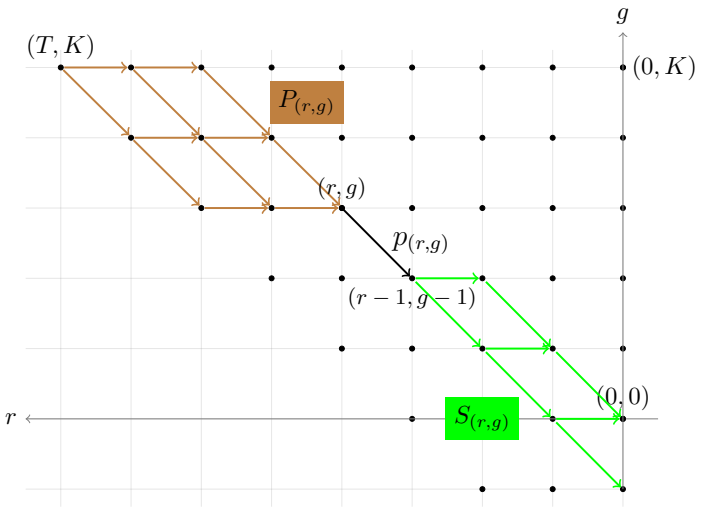

(ii) Conditional on $\mathcal{S}$

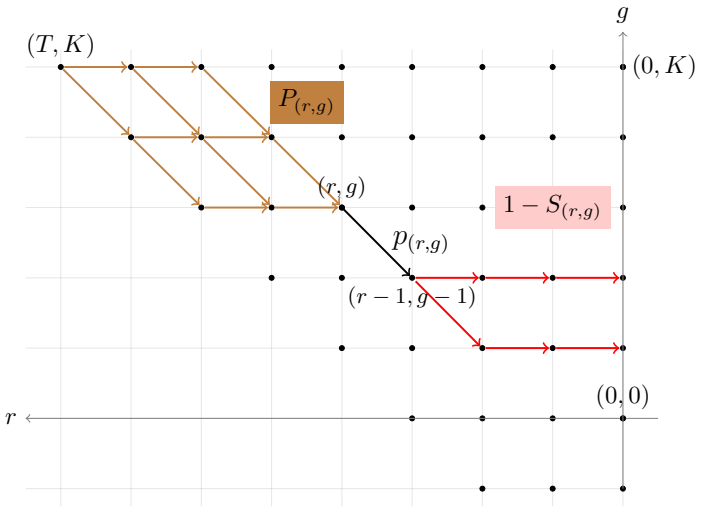

(iii) Conditional on $\mathcal{F}$

Simulation of gaps with homogeneous inspection costs ($T = 60$, $K = 25$, $q = .5$, $c = .25$)

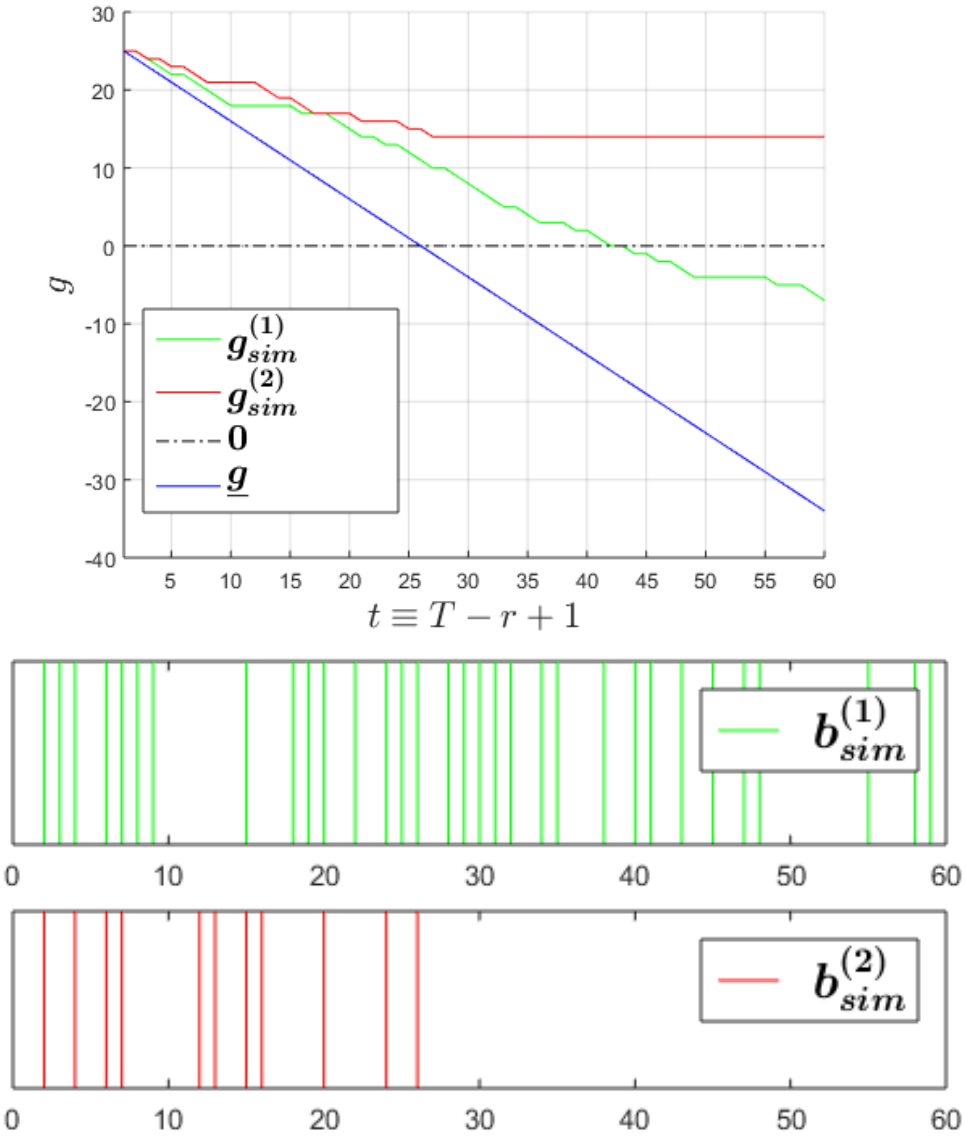

Simulated bids

Figure 13: Bid rates for the the example in Fig. 5

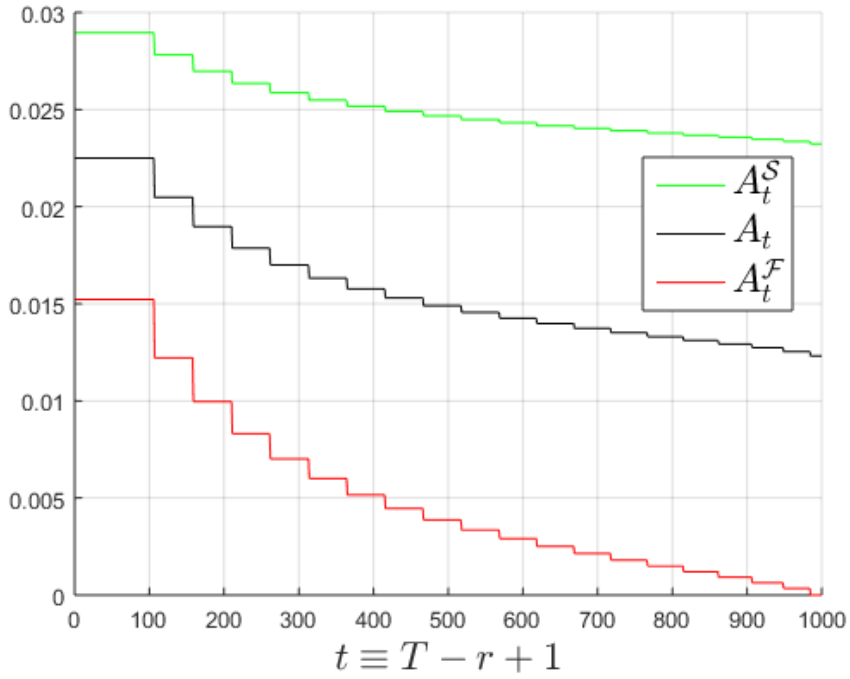

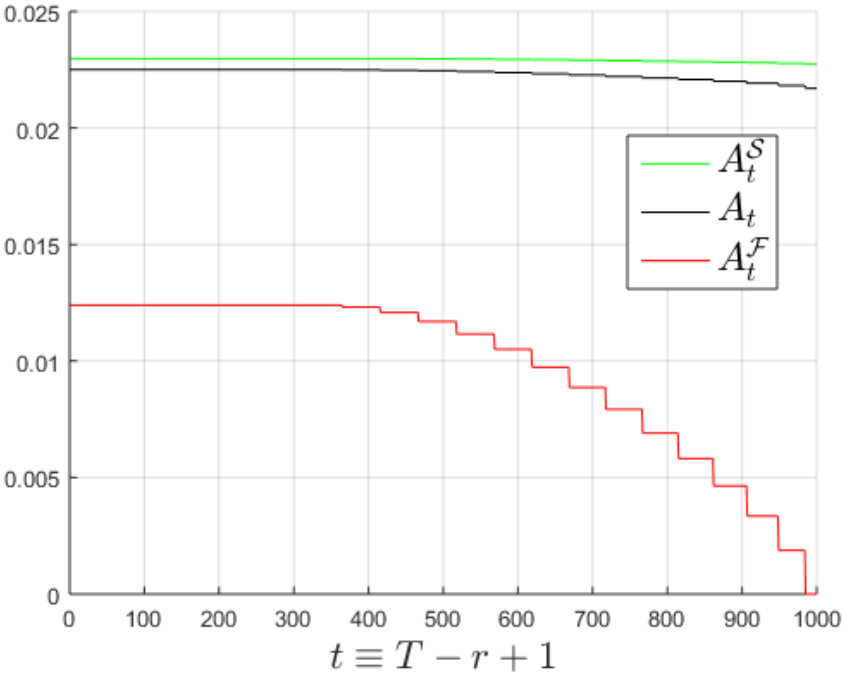

Figure 14: Bid rates for the the example in Fig. 7

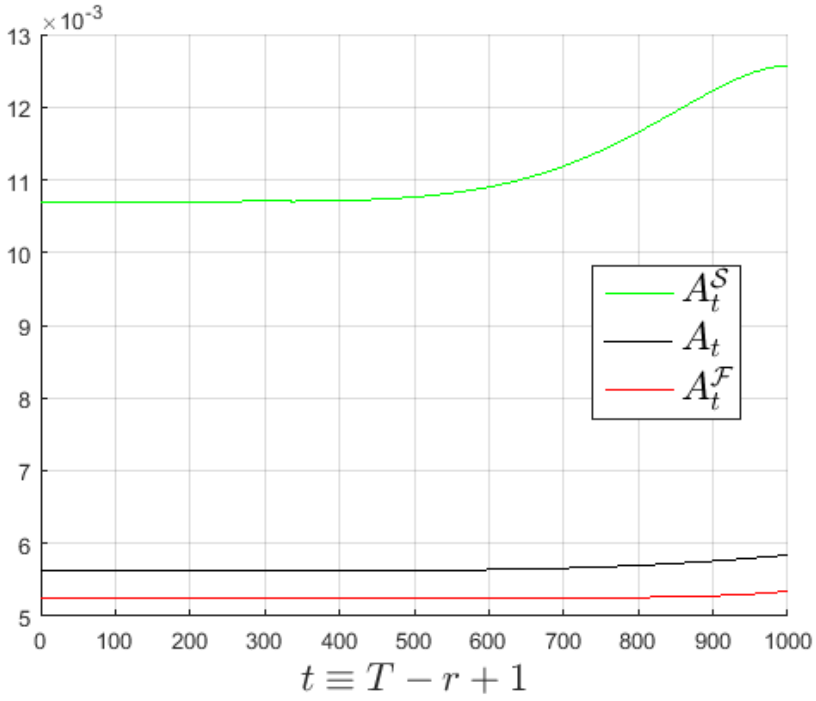

Figure 15: Bid rates for the the example in Fig. 9